

For Reference

NOT TO BE TAKEN FROM THIS ROOM

THE HYPERFINE STRUCTURE
OF SOME HIGHER TERMS OF THE SPECTRUM
OF SINGLY IONIZED THALLIUM

by

Albert Prebus, B.Sc.

UNIVERSITY OF ALBERTA, 1937.

EX LIBRIS
UNIVERSITATIS
ALBERTAENSIS



I N D E X

	Page
1. Introduction	1
2. Theory of Hyperfine Structure	7
3. Apparatus and Experimental Procedure	27
4. Experimental Results and Discussion	50
5. Acknowledgments	68

- 1 -

INTRODUCTION.

The field of modern atomic physics is mainly a study of the constitution of the atomic nucleus, the electro-magnetic properties of its constituent particles and their behavior when interacting with each other. A great deal of information concerning the behavior of bound electrons, such as the extra-nuclear electrons of an atom, has been gained from a thorough study of the line spectra of the elements. It is hoped that the laws of motion and interaction of electrons thus derived may be carried over into the field of nuclear physics to furnish a reasonably complete explanation of the observed phenomena associated with the nucleus. Considerable progress has already been made along these lines.

Of late years the domain of spectroscopy has been extended to the field of nuclear physics. With the development of optical instruments of high resolution, it became evident that many atomic spectrum lines were not single as expected, but consisted of a number of components. This hyperfine structure was not amenable to explanation in terms of a theory which regarded the atomic nucleus merely as a massive charged particle. Concurrently with quantitative measurements of this hyperfine structure, theories of its cause were



Digitized by the Internet Archive
in 2018 with funding from
University of Alberta Libraries

formulated. It was soon recognized that a study of hyperfine structure might provide a fruitful source of knowledge concerning the properties of the nucleus. Although nothing about the nuclear constitution can be learned from hyperfine structure, values of its total mechanical angular momentum and magnetic moment may be deduced. The numerical values of these two properties form a critical test for a theory of nuclear constitution.

At present there are three effects in terms of which the main features of hyperfine structure are explained. If an element is comprised of more than one Isotope, each will give rise to an atomic spectrum which may differ slightly from that of the others. This is termed the isotope displacement effect. By including in the Hamiltonian of the atomic system the kinetic energy of the nucleus there result two types of displacement in the energy levels. One is due to a change in the Rydberg constant, and is the same for all levels. The effect is only observable in the case of light elements, most markedly in hydrogen (a). The other type of displacement varies from term to term and may be traced to a set of terms in the Hamiltonian representing an interaction between the momenta of the extra-nuclear electrons (b). The consequences of this

(a) For photographs and discussion see White
INTRODUCTION TO ATOMIC SPECTRA p.35 and seq.

(b) Condon and Shortley THE THEORY OF ATOMIC
SPECTRA p.419.

effect for the two neon isotopes has been worked out by Bartlett and Gibbons (c). They found that the theoretical displacement of the energy levels, although in the right direction, were much smaller than the observed shifts.

A second reason for isotope structure is a deviation from the Coulomb law in the region near the nucleus. By assuming nuclei of finite radius which varies with the atomic weight, Racah, Rosenthal and Breit (d) have had some success in explaining large isotope displacements such as occur in thallium. Recently Schüßler and Schmidt (e) have also considered the effects on the levels of single isotopes of deviations from spherical symmetry of the nuclear field. However, many outstanding discrepancies still remain which throw doubt upon the assumptions and methods of theoretical predictions.

The second type of structure, which is called hyperfine structure to distinguish it from isotope structure, occurs in elements which have but one isotope. Pauli (f) suggested that this was due to the existence of a nuclear angular momentum with an associated magnetic moment.

(c) Bartlett and Gibbons - Phys. Rev. 44, 538, (1933)

(d) Racah - Nature 129, 723 (1932)
 Rosenthal and Breit - Phys. Rev. 41, 459, (1932)
 Breit - Phys. Rev. 42, 348, (1932)

(e) Schüßler and Schmidt - Zeit.f. Physik 94, 457, (1935)
 " " 98, 430, (1936)

(f) Pauli, W. - Naturwissenschaften 12, 741, (1924)

Successful theoretical interpretations have been made on the basis of this assumption so that it is at present possible to deduce the numerical values of these moments from a knowledge of the hyperfine energy level separations of the atom in question. To determine energy level separations of an atom it is necessary to measure the wave-number separations of the components of its spectrum lines. It is the object of this investigation to determine a number of energy level separations of singly-ionized thallium (Tl II) and from some of these to evaluate its nuclear magnetic moment.

The hyperfine structure of Tl II has been of interest because of its simplicity and the magnitude of the separations to be measured. Also, its term analysis is fairly complete, through the efforts of a number of investigators (g). The hyperfine structure of some of the lines were observed by the above. McLennan and Crawford (h), from an observation of the intensities and separations of the hyperfine components of some of the lines, deduced the value of the mechanical moment of thallium. Schüller and Keyston (i) and later

- (g) Rao, Narayan and Rao - Indian Journ. Phys. 2, 467, (1928)
McLennan, McLay and Crawford - Trans. Roy. Soc. Can. 22, 241, (1928).
Proc. Roy. Soc. A125, 570, (1929).
Smith - Proc. Nat. Acad. Sci. 14, 951, (1928).
Phys. Rev. 35, 235, (1930).
Ellis and Sawyer - Phys. Rev. 49, 145, (1936).
A table of all known terms and classified lines is contained in this paper.

(h) McLennan and Crawford - Proc. Roy. Soc. A132, 10, (1931)

(i) Schüller and Keyston - Zeit. f. Physik, 70, 1, (1931)

Smith and Convey (j) greatly extended the analysis with improved accuracy, the latter (j) calculating a number of values for the magnetic moment. In the investigations of both of the above, many large isotope displacements were observed.

Previous investigators have been concerned with those spectrum lines associated with the lower terms of Tl II. In the type of light source used in interferometer work, lines associated with the higher terms are generally fainter. Unfortunately, it is a custom to choose only the strongest and most easily accessible lines of a spectrum first, and neglecting those which entail more experimental difficulty; even though they are equally interesting from a theoretical point of view. Since a considerable amount of data on thallium has already been accumulated, it was considered worthwhile to extend this to higher terms so that a comparison of the structure of a number of terms of the same kind and belonging to the same spectrum would be possible. In the case of Tl II many of these lines are in a rather difficult region of the spectrum. Some of these, in the region $2600\text{\AA} - 3250\text{\AA}$ were investigated with the use of the quartz Lummer - Gehrke plate. As only plane - polarized light may be used with an interferometer of this type, an added difficulty was met with. A

(j) Smith and Convey - Can. Journ. of Research A14, 139, (1936)

Nicol prism, which may be used to eliminate one of the plane-polarized components, was found to absorb effectively all radiation below 3200\AA . Consequently, a Wollaston prism had to be used. This separates the two component vibrations by only a small angle, instead of absorbing one as does the Nicol. When the two images of the light source are formed, they overlap almost completely. Only the light forming that part of one image clear of the other can be used. This greatly reduces the amount of light acting on the photographic emulsion, so that exposures of from ten to forty hours' duration were required. Considerable difficulty was encountered in maintaining the strength of the light source throughout these long periods, as well as in keeping other conditions, mainly the temperature of the optical apparatus, unaltered.

THEORY OF HYPERFINE STRUCTURE

The fundamental postulate (f) of the present theory of the hyperfine structure of atomic energy levels is the existence of a nuclear angular momentum with an associated co-directed magnetic moment. We shall denote these vectors by \vec{I} and $\vec{\mu}$ respectively and connect them by the relation

$$\vec{\mu} = \frac{g(I) \cdot e}{1838} \frac{h}{2mc} \vec{I} \dots\dots\dots(1)$$

where $g(I)$ - the nuclear g factor

$$\frac{1}{1838} = \frac{m}{M} \text{ - ratio of mass of electron to that of proton.}$$

and the universal constants e, h, m, c have the conventional meanings
 e -electronic charge
 h -Planck's constant
 m -electronic mass
 c -velocity of light.

The vector \vec{I} is defined quantum - mechanically as is the general atomic angular momentum vector \vec{J} (ref. (k) eqn.3, p.46) Eigenvalues of \vec{I}^2 and any one component I_z are

$$I(I+1) \frac{h^2}{4\pi^2} \text{ where } I \text{ is any integer or half-integer.}$$

and
$$\frac{Mh}{2\pi} \text{ where } M_z \text{ is integral or half-integral as } I \text{ is integral or half-integral.}$$

M_z has the range of values

$$I, I-1, I-2, \dots\dots\dots -(I-1), -I.$$

The values of I for the elements of odd atomic weight have been found to be half-integral (k) p. 424. and zero for elements of even atomic weight.

(k) Condon and Shortley - THEORY OF ATOMIC SPECTRA (1935)

The magnetic moment of the nucleus gives rise to a magnetic field with which the extra-nuclear electrons interact. The resultant interaction can be divided into two parts, one of which is associated with all the electrons in closed shells. This is constant for all energy levels and hence may be disregarded. The other part, associated with the valence or optical electrons causes the splitting of the ordinary fine-structure multiplet levels into hyperfine levels. For the purpose of the following theoretical calculations it will be assumed that the nuclear interaction energy is small as compared to the energy of electrostatic and spin-orbit interactions. An expression for the nuclear interaction energy H' has been adopted in the form

$$H' = \alpha \vec{I} \cdot \vec{J} \dots \dots \dots (1)$$

where α is a constant for a given fine structure multiplet or J level and the vector \vec{J} represents the total angular momentum of all the optical electrons. This energy is then considered as a small perturbation on the J levels. Actually, the assumption that H' is small is not always valid and there occur discrepancies between theory and experiment which can be explained by treating the nuclear interaction (1) on an equal footing with the spin-orbit interaction. Goudsmit and Bacher (2) have carried through detailed calculations of this kind for the case of the anomalous levels of mercury and aluminum.

(2) Goudsmit and Bacher - Phys. Rev. 43, 894, (1933).

In the following pages methods of evaluating the intervals between hyperfine levels by use of the expression (1) will be indicated. As the calculations are rather complex, the results for the case of a one valence electron atomic system will be partly quoted in section (A). In section (B) the results of (A) will be used in the calculations of a two electron system.

(A) Single Electron System.

Neglecting nuclear interaction, the energy levels of a single electron system in the absence of an external field are characterized by the set of quantum numbers (q.nos.) n, l, j, m_j, I, M_I , where

n -- The total q.no. of the valence electron.

l -- the orbital angular momentum q. no.

j -- $(l \pm \frac{1}{2})$ - the total angular momentum q.no.

m_j -- the q.no. of any one component of the vector \vec{J} customarily the z component J_z .

I -- the nuclear angular momentum q.no.

M_I -- the q.no. of the z component of the vector I .

The energy levels are degenerate in or independent of the values of m_j and M_I or any other quantum numbers derived from these two. Including the weak interaction (1) in the Hamiltonian of the system removes part of this degeneracy, for each multiplet or j level is divided into several by its addition.

According to quantum-mechanical perturbation theory (ref. (k) chap.II), the eigenvalues of H' , or the displacements of the hyperfine levels from the unperturbed

j levels, are given by the diagonal elements of a matrix in which $H'_{\vec{I}, \vec{J}}$ is diagonal with respect to the quantum numbers representing the degeneracy in the unperturbed j levels i.e. a pair of quantum numbers derived from m_j, M_I . We define the vector \vec{F} as the total angular momentum of the atomic system, i.e. the sum

$$\vec{F} = \vec{I} + \vec{J}$$

It is defined quantum-mechanically as we define \vec{I} on page 7. As it is the sum of \vec{I} and \vec{J} , its quantum number f, will have the range of values

$$(I+J), (I+J-1), \dots, |I-J|.$$

and for any value of f, the quantum number m_f of any one component F_z of \vec{F} , will have the range of values

$$f, (f-1), (f-2), \dots, -f.$$

For a discussion of the addition of angular momentum vectors kindly see ref.(k) chap. 3, sec.6.

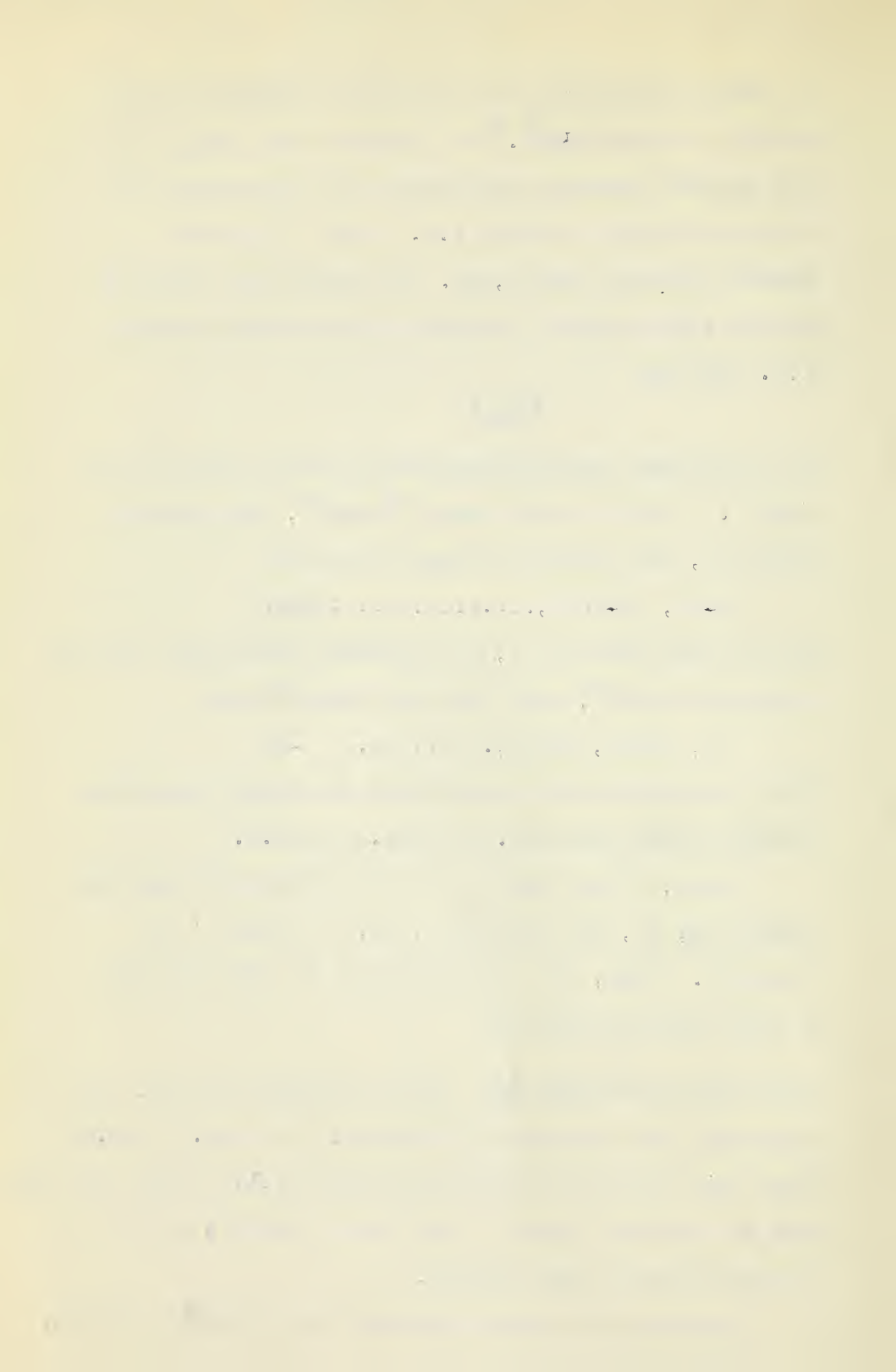
Hence, we may derive from the degenerate quantum numbers m_j, M_I , the numbers f, m_f , in which H' is diagonal. Thus, the eigenvalues of H' are given to a first approximation by

$$W(f) = (n l j f m_f | \alpha \vec{I} \cdot \vec{J} | n l j f m_f) \quad \text{in the notation of ref. (k)}$$

Comparing this expression with ref. (k) chap.II sec.9, note that we have co-related the set (n, l, j) with their n ; the quantum number f with their number l and the perturbation H' with their V .

Expanding the above expression as a matrix product, we have

$$W(f) = \sum_{n' l' j' f' m'_f} (n l j f m_f | \alpha | n' l' j' f' m'_f) (n' l' j' f' m'_f | \vec{I} \cdot \vec{J} | n l j f m_f)$$



Now $\vec{I} \cdot \vec{J}$ is diagonal in l, j, f, m_f , and the non-diagonal elements of $\vec{I} \cdot \vec{J}$ in n are neglected. Hence the product becomes

$$\begin{aligned} w(f) &= (n l j f m_f | \alpha | n l j f m_f) (n l j f m_f | \vec{I} \cdot \vec{J} | n l j f m_f) \\ &= (n l j f m_f | \alpha | n l j f m_f) \left[\frac{f(f+1) - I(I+1) - j(j+1)}{2} \right] \\ &= a(j) \left[\frac{f(f+1) - I(I+1) - j(j+1)}{2} \right] \dots \dots \dots (2) \end{aligned}$$

where $a(j)$ is the matrix element $(n l j f m_f | \alpha | n l j f m_f)$.

This element is independent of f and m_f , and we shall write its dependence on n, l, j in the form of ref. (k)

$$a(j) = (n l j; \alpha; n l j)$$

The eigenvalues of (2) are the displacements of the hyperfine or f levels from the unperturbed j levels. The form of (2) shows that the intervals between f levels obey the Landé interval rule, which reads in this case - - the interval between two adjacent f levels is proportional to the higher f value of the pair. Experimentally observed intervals generally follow this rule quite well. The observations of Smith and Beggs (m) on the spectrum of Bi II are a good example of its verification.

As shown by Fermi (n), the value of I may be deduced from the equation (2) by a measurement of the relative intensities of the components of a line for which either the initial or the final level has a small or zero hyperfine structure.

(m) - Smith and Beggs - Can. Journ. of Research 12, 690, (1935)

(n) - Fermi - Zeit. f. Physik 60, 320, (1930)

The theoretically difficult part of the problem is the evaluation of the constant $a(j)$ of (2). Hargreaves, Casimir, Goudsmit (o) and others have obtained values of $a(j)$ for the case of an electron whose l value is not zero. These values were obtained, non-relativistically, by treating the nucleus and optical electron simply as a pair of ^{charged} magnetic particles. For s electrons ($l=0$), an expression was derived by Fermi (n). By introducing the magnetic field due to the nucleus into the Dirac equation of the electron (p), Breit and Doermann (q) obtain ^{an} expressions ~~of H'~~ which is then used in the Schroedinger equation with the results of both Goudsmit (o) and Fermi (n). These calculations clearly indicate the nature of the approximations involved. As shown by Goudsmit (o), all of the above results agree poorly with experiment for various reasons. Improved results were obtained by Breit and Wills (r), who made a complete relativistic calculation of the constants. We shall quote their values and apply them in later calculations. Equation (29.1), page 478 of ref. (r) is

$$a(j) = \frac{2g(1)}{1838} \frac{\mu^2 2(2+1)}{j(j+1)} \cdot \left(\frac{1}{r}\right) \cdot F / hc \quad cm^{-1} \dots (3)$$

- (o) - Hargreaves - Proc. Roy. Soc. A124, 568, (1928)
 Proc. Roy. Soc. Lond. A127, 407, (1930)
 Casimir - quoted in Pauling and Goudsmit
 STRUCTURE OF LINE SPECTRA, p. 208.
 Goudsmit - Phys. Rev. 37, 663, (1931)
- (p) Dirac - QUANTUM MECHANICS, p. 253.
- (q) Breit and Doermann - Phys. Rev. 36, 1732, (1930).
 Breit - Phys. Rev. 37, 51, (1931).

where F is the relativity correction to the results of Goudsmit (o) and is expressed by

$$F = \frac{2(j+\frac{1}{2})(j+1)(2j+1)}{\rho(4\rho^2-1)} \quad \text{where } \rho^2 = (j+\frac{1}{2})^2 - Z^2\alpha^2 = (j+\frac{1}{2})^2 - Z^2\left(\frac{2\pi e^2}{hc}\right)^2$$

Z = atomic number.

$\left(\frac{1}{r}\right)^2$ is the average value (quantum mechanical) of the inverse cube of the distance between the nucleus and 1 electron.

$\mu_B = \frac{eh}{4\pi mc}$ the Bohr magneton.

In the case of an s electron (3) is meaningless and we use the expression of Fermi with a relativity correction (as given by Racah (s) eqns. (4) and (8))

$$a(s) = \frac{16\pi}{3} \cdot \frac{g(I)}{1838} \frac{\mu_B^2}{hc} \psi^2(0) \cdot F \dots f \dots (4)$$

where F is the relativity correction as above,

$\psi^2(0)$ - is the value, at the center of the nucleus, of the Schroedinger eigenfunction.

It may be pointed out here that this expression for F differs from Racah's eqn. (8) for non-s electrons. In his expression the factor $2(2j+1)$ of F above, is replaced by $4j$. The two expressions agree for l electrons when $j = l + \frac{1}{2}$, but differs when $j = l - \frac{1}{2}$. It is impossible to form an opinion as to which is more correct since Racah's result is not derived in his paper. In comparing these expressions with Racah, note must be taken of the fact that his symbols a_j are to be divided by l_j to make them agree with ours.

Breit and Wills obtain a new coefficient a''' , to be defined later, which will be useful when we consider the problem of two electrons. This is

(r) Breit and Wills - Phys. Rev. 44,470, (1933)

(s) Racah - Zeit. f. Physik 71,431, (1931).

(eqn. 29.2 of ref. (r))

$$a''' = - \left[\frac{3 \mu_0^2}{27+1} \cdot \left(\frac{1}{r^3} \right) \right] \frac{G}{hc} c m^{-1} \dots \dots \dots (5)$$

where $G = \frac{22(\ell+1)}{\pi Z^2 \alpha^2} \sin \pi \left[\sqrt{1-2\alpha^2} - \sqrt{1-2\alpha^2} \right]$ (eqn. (27.1) of ref. (r))

In these formulae (3), (4), (5), the unknowns $\psi^{(0)}$ and $\left(\frac{1}{r^3} \right)$ must be evaluated. Racah obtained $\psi^{(0)}$ by a statistical method and $\left(\frac{1}{r^3} \right)$ is obtained from fine structure data as follows.

The total fine structure splitting of an **2** doublet is given by the expression

$$\Delta W = \left(\frac{2\ell+1}{2} \right) \mathfrak{F}_1 c m^{-1} \quad (\text{see ref. (k) p.122 eqn. (7)}) \dots (6)$$

$$\text{where } \mathfrak{F}_1 = \frac{h^2}{4\pi^2} \int_0^\infty R^2(r) \frac{1}{2m^2 c^2} \left(\frac{1}{r} \frac{\partial U(r)}{\partial r} \right) \cdot dr / hc \quad c m^{-1}$$

in which $R(r)$ is the radial part of the Schrodinger eigenfunction of the **nl** configuration and $U(r)$ is the potential energy of the **2** electron in the electric field of the nucleus.

We may reduce \mathfrak{F}_1 to the form

$$hc \mathfrak{F}_1 = \frac{2}{e^2} \mu_0^2 \left(\frac{1}{r} \frac{\partial U(r)}{\partial r} \right) \dots \dots \dots (7)$$

and in a hydrogenic case

$$\left(\frac{1}{r} \frac{\partial U(r)}{\partial r} \right) = Z e^2 \left(\frac{1}{r^3} \right) \dots \dots \dots (8)$$

We make the approximation (8) for a non-hydrogenic atom. This approximation introduces an error, in that Z should be replaced by a number less than the atomic number. Eqn. (8) implies that the **2** electron is not screened from the nucleus by those electrons in closed shells. This is discussed by Fermi and Segré(t). The value of \mathfrak{F}_1 can be inferred from the fine structure separation and hence we have approximately

$$\overline{\left(\frac{1}{r^3} \right)} = \frac{\mathfrak{F}_1 hc}{2 Z \mu_0^2}$$

(t) Fermi and Segré- Zeit.f.Physik 82,732, (1933)

Introducing the relativity correction ~~H~~ ~~and Racah~~ (s) (Racah's expression (10)) we have finally

$$\overline{\left(\frac{1}{r^3}\right)} = \frac{3\epsilon}{2\pi\mu^2} \frac{hc}{H} \dots\dots\dots (9)$$

$$\text{where } H = 2 \frac{\sqrt{(2+1)^2 - 2\alpha^2} - 1 - \sqrt{(2-2\alpha^2)} \cdot 2(2+1)}{2^2 \alpha^2}$$

The methods indicated for obtaining values of $\psi^{(0)}$ and $\overline{\left(\frac{1}{r^3}\right)}$ have been found to give inconsistent results. For a single electron spectrum, better results may be obtained by the use of semi-empirical formulae as discussed by Goudsmit in a later paper (u). However, we shall use the above results for a two electron system, for it is difficult to see how to determine the necessary constants in Goudsmit's formulae (eqns. (5) and (6) ref. (u)).

(B) Interaction Constants for a Two Electron System.

When there are more than one optical electrons in the atomic system, calculations of the interaction energies become more involved. Neglecting nuclear spin interaction, the energy levels of an atom are still characterized by a quantum number J representing the total angular momentum of all the optical electrons. The effect of a nuclear interaction, as in the one electron spectrum, is to split the J levels into a number of components. We shall show that the splitting conforms to the Landé interval rule or eqn. (2) of the previous section. The object of this section is

to evaluate the constant a_0 of (2) for a two electron system in terms of the one electron constants.

Following the method of Breit and Wills (r), we shall carry through the calculations for a pair of electrons with the configuration label $(ns, n'l)$ or simply (s, l) .

The states of the configuration (s, l) are characterized by the set of quantum numbers $ns, n'l$ specifying the configuration; a set of quantum numbers which specify the type of coupling, i.e. the relative magnitudes of the electrostatic and spin-orbit interactions - - we shall denote this set at present by the single symbol γ ; the numbers J and M_J to which we add the nuclear spin quantum number I and M_I of p.7. Provided the nuclear interaction is small, the unperturbed levels of such a system will always be characterized by J .

If the coupling is extreme (jj) or (LS) then the symbol γ will represent the j 's of the individual electrons, or their resultant L and S , respectively. Generally the coupling is not extreme and the states of the system may be approximately expanded in terms of the (jj) or (LS) coupled states, depending on whether the coupling is nearly (jj) or (LS) respectively. Thus we may represent a state in intermediate coupling either as

$$\Psi(\gamma J M_J) = \sum_{\gamma s} c_{\gamma s} \Psi(j_1 j_2 \dots J M_J) \dots \dots \dots (10)$$

where $\Psi(j_1 j_2 \dots J M_J)$ is the (jj) coupled state belonging to $J M_J$

$$\text{or as } \Psi(\gamma J M_J M_I) = \sum_s K_s \varphi(L_s S_s J M_J M_I) \dots\dots\dots (11)$$

where $\varphi(L S J M_J M_I)$ is the (LS) coupled state belonging to $J M_J M_I$

and a determination of the constants c_s , K_s defines the state in question.

Since the one electron constants, eqns. (3)(4)(5), depend upon the j values of the individual electrons, it will be necessary to make preliminary calculations with the ($j j$) coupled states of (10).

For the eigenstates of the level $J=2$ of the $s1$ configuration the expansion (10) is

$$\Psi(\gamma J M_J M_I) = c_1 \psi(\frac{1}{2}, 2 + \frac{1}{2}, J, M_J M_I) + c_2 \psi(\frac{1}{2}, 2 - \frac{1}{2}, J, M_J M_I) \dots\dots (12)$$

where the $\frac{1}{2} = j$, of s electrons

$1 \pm \frac{1}{2} = j$ of 1 electron.

We regard the interaction energy H' for the two electron system as the sum of the interactions of the individual electrons, and write

$$H' = \alpha(s) \vec{I}_s \cdot \vec{J}_s + \alpha(1) \vec{I}_1 \cdot \vec{J}_1 \dots\dots\dots (13)$$

To find the eigenvalues of (13) we use the $\gamma, J, f m_f$ scheme as we did in sec. (A) and have

$$w(f) = (\gamma I J f m_f | \alpha(s) \vec{I}_s \cdot \vec{J}_s | \gamma I J f m_f) \dots\dots\dots (14) \\ + (\gamma I J f m_f | \alpha(1) \vec{I}_1 \cdot \vec{J}_1 | \gamma I J f m_f)$$

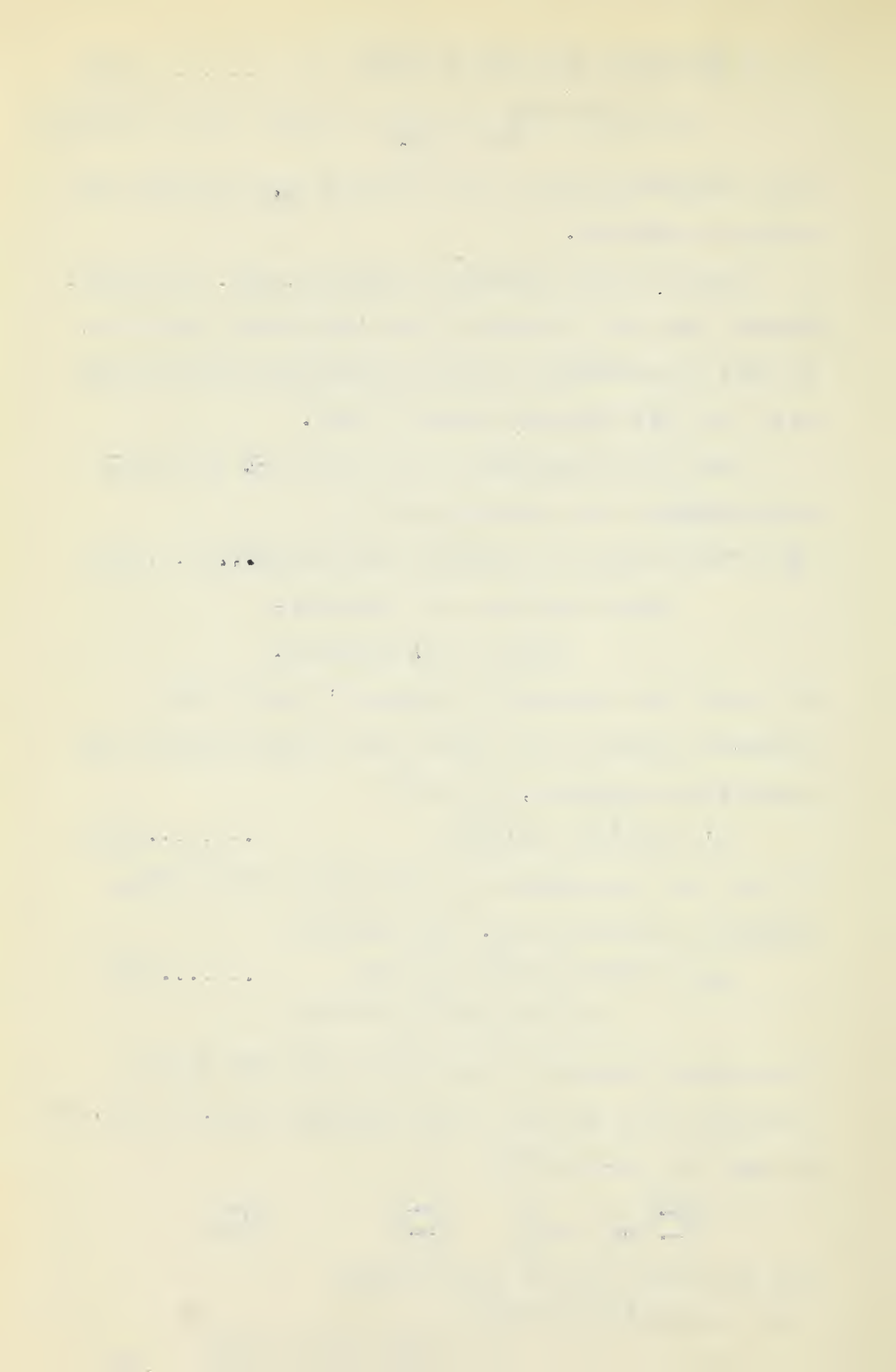
The matrix elements on the right hand side may be evaluated with the aid of the formulae of p.71, ref.(k)

We make the co-relation

$$\begin{array}{ccc} \vec{P} \rightarrow \vec{I} & j_1 \rightarrow J & j \rightarrow f \\ \vec{Q} \rightarrow \alpha(s) \vec{J}_s \text{ or } \alpha(1) \vec{J}_1 & j_2 \rightarrow I & m \rightarrow m_f \end{array}$$

For the first term of (14) we have

$$(\gamma I J f m_f | \alpha(s) \vec{I}_s \cdot \vec{J}_s | \gamma I J f m_f) \\ = \sum_{\gamma'} (\gamma I : I : \gamma' I) (\gamma' I : \alpha(s) J_s : \gamma J) \left[\frac{f(f+1) \cdot I(I+1) - J(J+1)}{2} \dots\dots \right] \dots\dots (15)$$



and for the second

$$(\gamma I J f m_f | \alpha(2) \vec{I} \cdot \vec{J}_2 | \gamma I J f m_f) \\ = \sum_{\gamma'} (\gamma I : I : \gamma' I) (\gamma' J : \alpha(2) J_2 : \gamma J) \left[f(f+1) - I(I+1) - J(J+1) \right] \dots (16)$$

In the eqns. (15) and (16) we have used the notation of ref. (k) to express the dependence of the matrix of I on the quantum numbers (γI) in the form

$$(\gamma I : I : \gamma' I)$$

and the dependence of the matrix of $\alpha(2) J_2$ on the quantum numbers (γJ) in the form

$$(\gamma' J : \alpha(2) J_2 : \gamma J)$$

Hence, by inspection of (15) and (16) we see that the whole dependence of H' on f is through the factor in braces.

Now the matrix element

$$(\gamma I J f m_f | \vec{F} \cdot \vec{I} | \gamma I J f m_f) = (\gamma I J f m_f | \frac{\vec{F}^2 - \vec{I}^2 - \vec{J}^2}{2} | \gamma I J f m_f)$$

Since $\vec{F}, \vec{I}, \vec{J}$ are diagonal in I, J, f, m_f , we have

$$(\gamma I J f m_f | \vec{F} \cdot \vec{I} | \gamma I J f m_f) = f(f+1) - I(I+1) - J(J+1) \cdot \frac{1}{4\pi^2}$$

Hence we may write (14) as

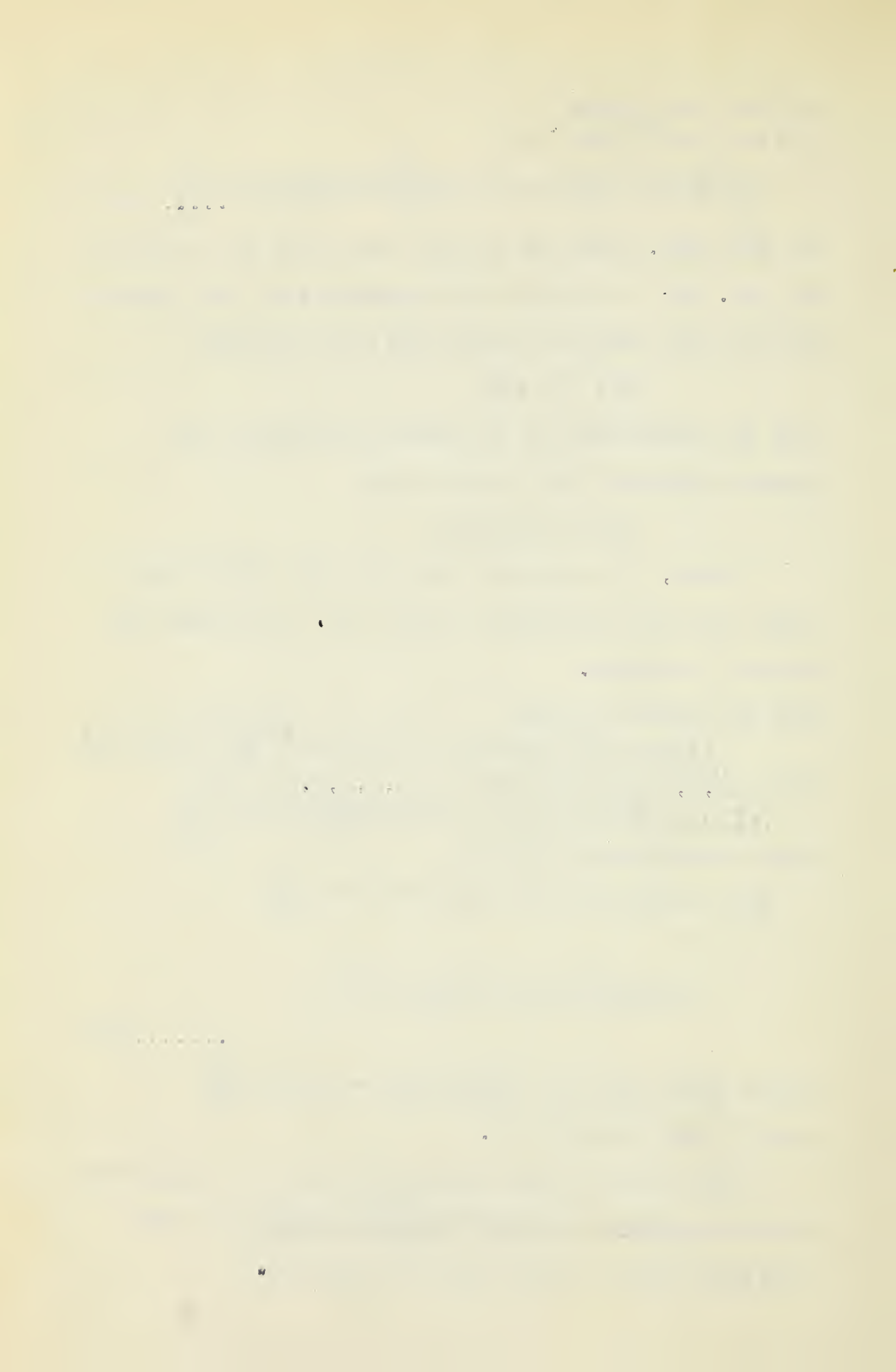
$$w(f) = A(IJ) (\gamma I J f m_f | \vec{F} \cdot \vec{I} | \gamma I J f m_f) \frac{1}{4\pi^2}$$

$$= A(IJ) \left[f(f+1) - I(I+1) - J(J+1) \right] \dots (17)$$

$$\text{where } A(IJ) = \sum_{\gamma'} (\gamma I : I : \gamma' I) \left[(\gamma' J : \alpha(2) J_2 : \gamma J) + \alpha(2) J_2 : \gamma J \right]$$

and is independent of f .

This result shows immediately that the hyperfine splitting, obeys the Lande interval rule for a two electron system in any type of coupling, \rightarrow



Let us now consider the evaluation of $A(IJ)$

of (17). By (17) it is evident that*

$$(\gamma I J M_J M_I | H | \gamma I J M_J M_I) = A(IJ) (\gamma I J M_J M_I | \vec{I} \cdot \vec{J} | \gamma I J M_J M_I) \frac{4\pi^2}{N} = A(IJ) M_I M_J$$

Expanding this matrix element in terms of (12) we have.

$$\begin{aligned} M_I M_J A(IJ) = & C_1^2 \left(\frac{1}{2} \gamma + \frac{1}{2}, J M_I M_J | H' | \frac{1}{2} \gamma + \frac{1}{2}, J M_I M_J \right) + C_1^2 \left(\frac{1}{2} \gamma - \frac{1}{2}, J M_I M_J | H' | \frac{1}{2} \gamma - \frac{1}{2}, J M_I M_J \right) \\ & + \bar{C}_1 C_2 \left(\frac{1}{2} \gamma + \frac{1}{2}, J M_I M_J | H' | \frac{1}{2} \gamma - \frac{1}{2}, J M_I M_J \right) \\ & + C_1 \bar{C}_2 \left(\frac{1}{2} \gamma - \frac{1}{2}, J M_I M_J | H' | \frac{1}{2} \gamma + \frac{1}{2}, J M_I M_J \right) \dots \dots \dots (18) \end{aligned}$$

The coefficients of the c's are readily determined.

We shall denote the coefficient of $\bar{C}_1 C_2$, by N, and

evaluate it as an example of the procedure.

$$\begin{aligned} N = & \left(\frac{1}{2} \gamma + \frac{1}{2}, I J, M_I M_J | \alpha(s) \vec{I} \cdot \vec{J} | \frac{1}{2} \gamma - \frac{1}{2}, I J M_I M_J \right) + \left(\frac{1}{2} \gamma + \frac{1}{2}, I J, M_I M_J | \alpha(t) \vec{I} \cdot \vec{J} | \frac{1}{2} \gamma - \frac{1}{2}, I J, M_I M_J \right) \\ = & \left(\frac{1}{2} \gamma + \frac{1}{2}, I : I : \frac{1}{2} \gamma + \frac{1}{2}, I \right) \left(\frac{1}{2} \gamma + \frac{1}{2}, J : \alpha(s) J s : \frac{1}{2} \gamma - \frac{1}{2}, J \right) M_I M_J \\ & + \left(\frac{1}{2} \gamma + \frac{1}{2}, I : I : \frac{1}{2} \gamma + \frac{1}{2}, I \right) \left(\frac{1}{2} \gamma + \frac{1}{2}, J : \alpha(t) J_t : \frac{1}{2} \gamma - \frac{1}{2}, J \right) M_I M_J \end{aligned}$$

This expansion is the same as used in eqns. (15) and

(16) with the substitution of $\frac{1}{2}$ and $I - \frac{1}{2}$ for γ . The

first term is zero since \vec{J}_s commutes with \vec{J}_t , and the

factor depending on I in the second term is unity.

$$\therefore N = M_I M_J \left(\frac{1}{2} \gamma + \frac{1}{2} : \alpha(t) J_t : \frac{1}{2} \gamma - \frac{1}{2} \right) \frac{\sqrt{P(\frac{1}{2}) Q(\frac{1}{2})}}{2 \gamma (\gamma + 1)} \text{ by eqns. 8, p. 69, ref. (k)}$$

$$\begin{aligned} \text{where } P(\frac{1}{2}) &= 4 \gamma (\gamma + 1) \\ Q(\frac{1}{2}) &= 1 \end{aligned} \quad \left\{ \begin{array}{l} \text{Note that } j \text{ of ref. (k) is } \gamma \text{ here.} \\ j_1 \quad \quad \quad \frac{1}{2} \\ j_2 \quad \quad \quad \gamma + \frac{1}{2} \end{array} \right.$$

$$\begin{aligned} \therefore N &= M_I M_J \left(\frac{1}{2} \gamma + \frac{1}{2} : \alpha(t) J_t : \frac{1}{2} \gamma - \frac{1}{2} \right) \frac{2 \sqrt{2(\gamma + 1)}}{2 \gamma (\gamma + 1)} \\ &= M_I M_J a \frac{\sqrt{2(\gamma + 1)}}{2(\gamma + 1)} \quad \text{where } \left(\frac{1}{2} \gamma + \frac{1}{2} : \alpha(t) J_t : \frac{1}{2} \gamma - \frac{1}{2} \right) = a''' \text{---see eqn. (5).} \end{aligned}$$

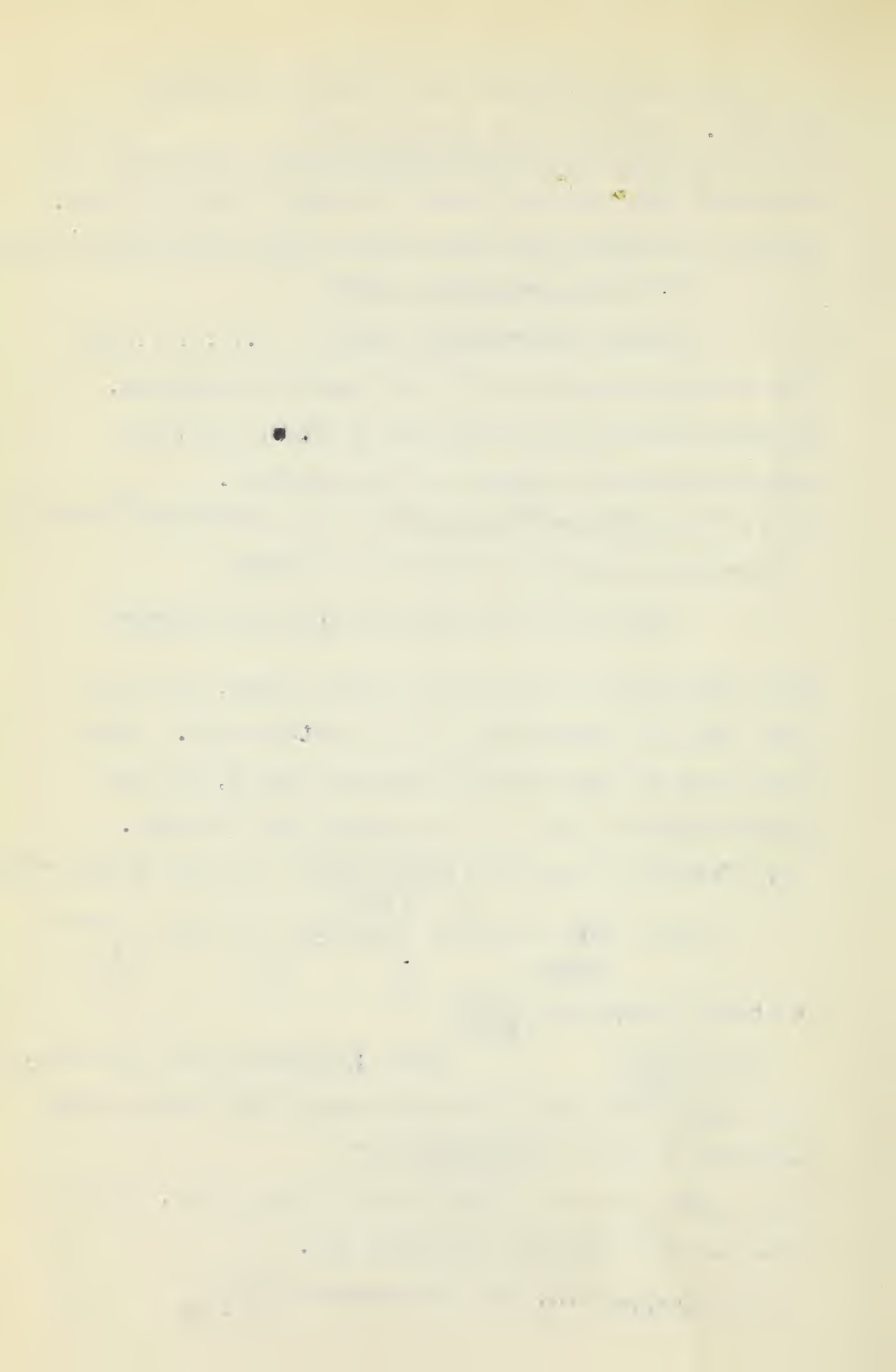
The coefficient of $C_1 \bar{C}_2$ is the same so that adding them

$$\text{together we have } \frac{2 M_I M_J \sqrt{2(\gamma + 1)}}{\gamma (\gamma + 1)} a'''$$

This agrees with the result of Breit and Wills, but is

obtained in a slightly different way.

* See ref. (k) p. 59 at top eqn. 3 with correlation $\begin{pmatrix} I \rightarrow S \\ J \rightarrow L \end{pmatrix}$



Hence, the final result for (18) is

$$\begin{aligned} \gamma(\gamma+1)A(I) = & \frac{1}{2}[\gamma(\gamma+1)c_1^2 - \gamma c_2^2]a(s) + \frac{1}{2}[\gamma(2\gamma+3)c_1^2]a(\gamma+\frac{1}{2}) \\ & + \frac{1}{2}(\gamma+1)(2\gamma-1)c_2^2 a(\gamma-\frac{1}{2}) + 2[\gamma(\gamma+1)]^{\frac{1}{2}} c_1 c_2 a'' \dots\dots\dots(19) \end{aligned}$$

We recall that this is for $J=1$.

The coefficients c_1, c_2 determining the two states of the same J will satisfy the relations

$$c_1^2 + c_2^2 = 1 \dots\dots\dots(20)$$

$$\begin{aligned} \text{and } \Psi_1(\gamma, J=1) &= c_1 \psi_1 + c_2 \psi_2 \\ \Psi_2(\gamma, J=1) &= c_2 \psi_1 - c_1 \psi_2 \dots\dots\dots(21) \end{aligned}$$

where the ψ_1, ψ_2 are the same as in (12).

If we add the A 's for the two J levels with due regard to (20) and (21), we obtain

$$\gamma(\gamma+1)(A_1 + A_2) = \frac{1}{2}a(s) + \frac{1}{2}\gamma(2\gamma+3)a(\gamma+\frac{1}{2}) + \frac{1}{2}(\gamma+1)(2\gamma-1)a(\gamma-\frac{1}{2}) \dots\dots(22)$$

Substituting into this expression, regarding F for the moment as a constant independent of j , the values

$$\begin{aligned} a(s) &= \frac{16}{3}\pi g \mu_0^2 \frac{\psi^2(0)}{1838hc} \cdot F \text{ cm}^{-1} \\ a(\gamma+\frac{1}{2}) &= 2g \mu_0^2 \frac{\gamma(\gamma+1)}{(\gamma+\frac{1}{2})(\gamma+\frac{3}{2})} \cdot \left(\frac{1}{\gamma}\right) \cdot F = \frac{8\gamma(\gamma+1)}{(2\gamma+1)(2\gamma+3)} \cdot \frac{g \mu_0^2}{1838hc} \left(\frac{1}{\gamma}\right) \cdot F \text{ cm}^{-1} \\ a(\gamma-\frac{1}{2}) &= 2g \mu_0^2 \frac{\gamma(\gamma+1)}{(\gamma-\frac{1}{2})(\gamma+\frac{1}{2})} \cdot \left(\frac{1}{\gamma}\right) \cdot F = \frac{8\gamma(\gamma+1)}{(2\gamma-1)(2\gamma+1)} \cdot \frac{g \mu_0^2}{1838hc} \left(\frac{1}{\gamma}\right) \cdot F \text{ cm}^{-1} \end{aligned}$$

we obtain

$$\gamma(\gamma+1)(A_1 + A_2) = \left\{ \frac{8}{3}\pi \psi^2(0) + \left[4\gamma(\gamma+1) \left(\frac{\gamma}{2\gamma+1} + \frac{\gamma+1}{2\gamma-1} \right) \right] \left(\frac{1}{\gamma}\right) \right\} \frac{g \mu_0^2}{1838hc} F$$

$$\text{and hence } (A_1 + A_2) = \left[\frac{8\pi}{3} \frac{\psi^2(0)}{\gamma+1} + 4\left(\frac{1}{\gamma}\right) \right] \frac{g \mu_0^2}{1838hc} \cdot F \text{ cm}^{-1}$$

The result agrees with Racah's equation (14), if note is made of the fact that his $a(j)$ must be divided by Ij to make it the same as ours.

By setting c_1, c_2 equal to zero, we get the value of A for the two J 's in the extreme case of (jj) coupling.

It is evident from the above summation that if Goudsmit's method of sums is used, the relativity correction F cannot be applied. This is generally not very important, for the relativity correction is small for 1 electrons.

In the expression (19), we have still to evaluate the coefficients c, c_2 . These can be obtained from a knowledge of the relative positions of the fine structure energy levels belonging to the s_l configuration. In the configurations to which we shall apply this theory the coupling is nearly (LS). Hence we must expand the $\bar{\Psi}(s, j, l, m)$ of the $^3L', ^1L'$ levels in terms of (LS) eigenfunctions. (We use the notation $^3L, ^1L$ for the levels which would be $^3L, ^1L$ if the coupling were strictly (LS)).

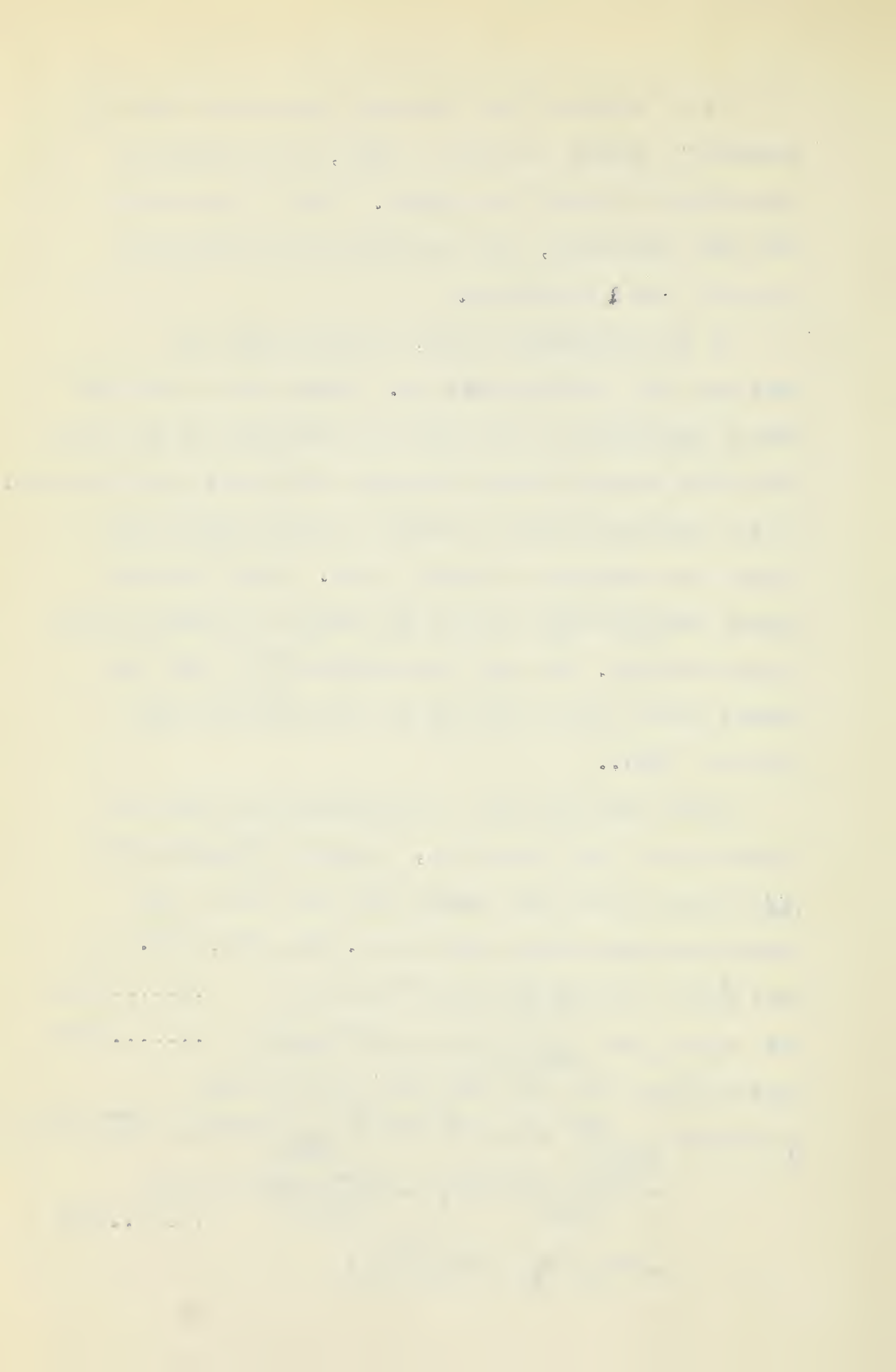
Since the A of (19) is determined in terms of constants of (jj) functions, we shall transform the (jj) states into (LS) states with the aid of the transformation matrix given on p. 294, ref. (k).

$$\text{Thus } \Psi(\frac{1}{2}, l + \frac{1}{2}, l, m_l) = \frac{1}{\sqrt{2l+1}} \left[\sqrt{l+1} \varphi(^1L_2) + \sqrt{l} \varphi(^3L_2) \right] \dots\dots\dots (23)$$

$$\text{and } \Psi(\frac{1}{2}, l - \frac{1}{2}, l, m_l) = \frac{1}{\sqrt{2l+1}} \left[-\sqrt{l} \varphi(^1L_2) + \sqrt{l+1} \varphi(^3L_2) \right] \dots\dots\dots (24)$$

Substituting (23) and (24) into (12) we have

$$\begin{aligned} \bar{\Psi}(s, l, m_l) &= \frac{c_1}{\sqrt{2l+1}} \left[\sqrt{l+1} \varphi(^1L_2) + \sqrt{l} \varphi(^3L_2) \right] + \frac{c_2}{\sqrt{2l+1}} \left[-\sqrt{l} \varphi(^1L_2) + \sqrt{l+1} \varphi(^3L_2) \right] \\ &= \frac{c_1 \sqrt{l+1} - c_2 \sqrt{l}}{\sqrt{2l+1}} \varphi(^1L_2) + \frac{c_1 \sqrt{l} + c_2 \sqrt{l+1}}{\sqrt{2l+1}} \varphi(^3L_2) \dots\dots\dots (25) \\ &= K_1 \varphi(^1L_2) + K_2 \varphi(^3L_2) \end{aligned}$$



where $K_1 = \frac{c_1 \sqrt{2l+1} - c_2 \sqrt{2}}{\sqrt{2l+1}}$ (26)

$K_2 = \frac{c_1 \sqrt{2} + c_2 \sqrt{2l+1}}{\sqrt{2l+1}}$

To determine the K's, we diagonalize the electrostatic plus spin-orbit interactions in the (LS) coupling scheme of states. In this scheme the electrostatic energy is already diagonal and the spin-orbit interaction matrix is given by ref. (k), page 268. Hence we obtain, in determinant form, the secular equation

	$^3L_{1,1}$	1L_1	3L_2	$^3L_{2-1}$		
$^3L_{1,1}$	$-2G_0 + \frac{1}{2}F_2 - \epsilon$				= 0	
1L_1		$-\epsilon$	$\frac{F_2}{2} \sqrt{2(l+1)}$		 (28)
3L_2		$\frac{F_2}{2} \sqrt{2(l+1)}$	$-2G_0 - \frac{1}{2}F_2 - \epsilon$			
$^3L_{2-1}$				$-2G_0 - \frac{F_2}{2}(l+1) - \epsilon$		

This factors into a chain of three equations

In this determinant the rows and columns are labelled by the (LS) quantum numbers. For example, the symbol 3L_1 represents the set of quantum numbers L, S=1, J=2. The symbol F_2 is the same as we have defined on page 14. It is twice the Landé interval factor for the L levels (ref. (k) p. 197) when the coupling is strictly (LS). Also $-2G_0$ is the energy difference of the 1L and center of gravity of the 3L terms when the coupling is (LS).

The determinantal equation above factors into a chain of three equations, one for each value of J.

Let $W(^1L_{2+})$ be root of equation for $J=2+$

$W(^1L'_2), W(^3L'_2)$ be roots of equation for $J=2$

$W(^3L_{2-})$ root of equation for $J=2-$

Then we have by inspection

$$\begin{aligned} W(^3L_{2+}) &= -2G_0 + \frac{1}{2}J_2 \\ W(^3L_{2-}) &= -2G_0 - \frac{1}{2}(2+1)J_2 \end{aligned} \quad \dots\dots\dots (29)$$

From (29) we easily derive the result

$$J_2 = \frac{2}{22+1} [W(^3L_{2+}) - W(^3L_{2-})] \quad \dots\dots\dots (30)$$

$$G_0 = - \frac{[(2+1)W(^3L_{2+}) + 2W(^3L_{2-})]}{2(22+1)} \quad \dots\dots\dots (31)$$

Thus, J_2 and G_0 are determined numerically from the experimental values of $W(^3L_{2+})$ and $W(^3L_{2-})$.

Substituting J_2 and G_0 into the secular equation (28) for $J=2$, we can solve for ϵ . The values of ϵ are then used in the equation

$$\frac{K_1}{K_2} = \frac{J_2 \sqrt{2(2+1)}}{\epsilon} \quad \text{to determine the constants } K_1, K_2 \dots\dots (31')$$

By means of (26) the ϵ 's are determined and used in (19).

This long and involved calculation is required to determine the $A(J)$ when there are two or more levels of the same J value in a configuration. When there is only one level belonging to a given J , the expansion (10) is simpler and for our sl configuration, consists of only one term for each of the J values $2+$ and $2-$. We get for the constants A in these two cases

* Absolute values are obtained from normalizing condition $K_1^2 + K_2^2 = 1$

$$J=2+1$$

$$A(^3L_{2+1}) = \frac{\alpha(s)}{2(2+1)} + \frac{22+1}{2(2+1)} \alpha(2+\frac{1}{2}) \dots\dots\dots (32)$$

$$J=2-1$$

$$A(^3L_{2-1}) = -\frac{\alpha(s)}{2} + \frac{22+1}{2} \alpha(2-\frac{1}{2}) \dots\dots\dots (33)$$

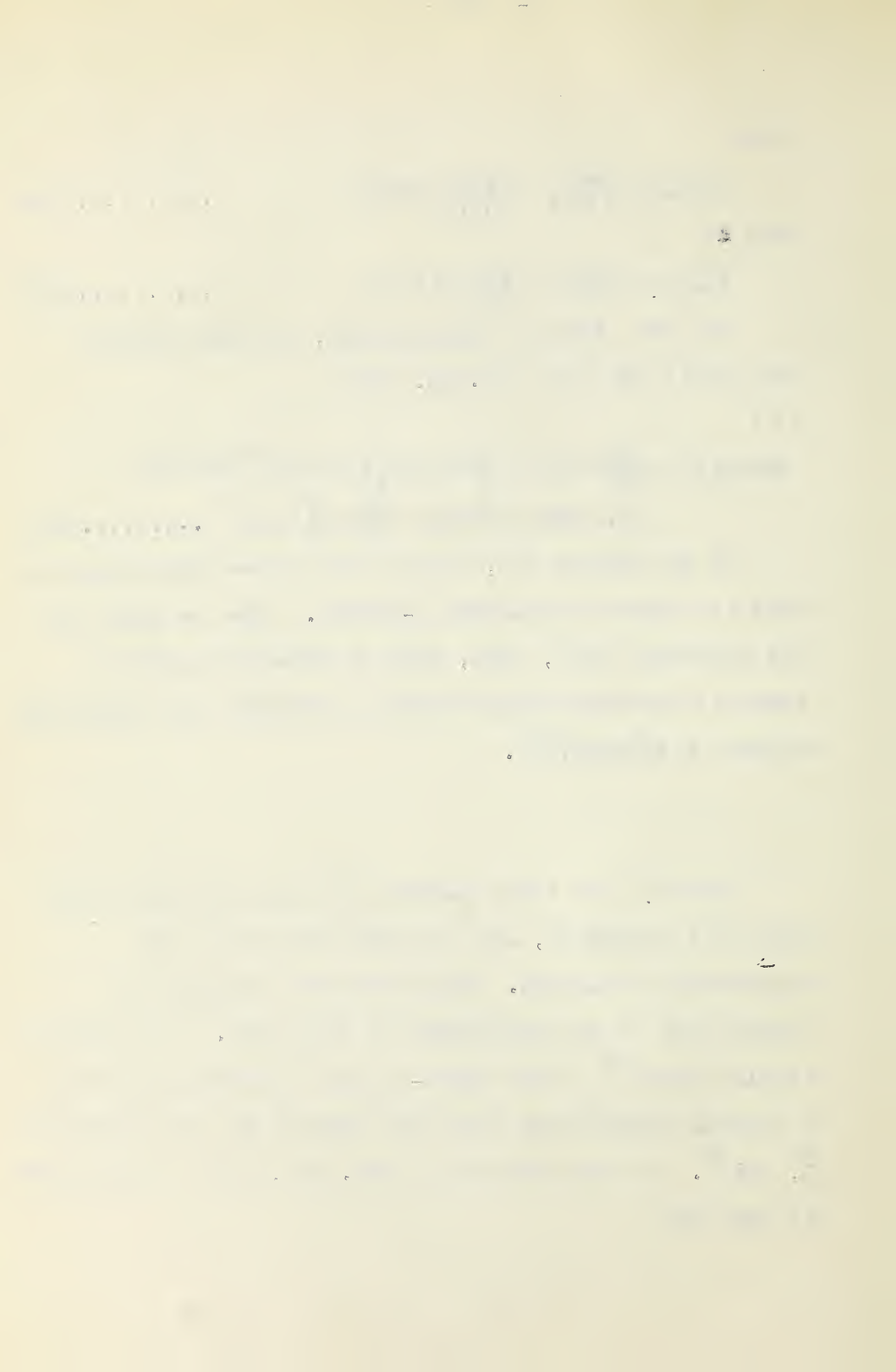
For the sake of completeness, we shall repeat the result for $J=2$ viz. eqn. (19)

$$J=2$$

$$\begin{aligned} 2(2+1)A(L_2) = & \frac{1}{2} \left[(2+1)c_2^2 - 2c_1^2 \right] \alpha(s) + \frac{1}{2} \left[2(22+3)c_1^2 \right] \alpha(2+\frac{1}{2}) \\ & + \frac{1}{2} (1+1)(22-1)c_2^2 \alpha(2-\frac{1}{2}) + 2 \left[2(2+1) \right] \frac{1}{2} c_1 c_2 \alpha''' \dots\dots\dots (34) \end{aligned}$$

If we examine (3), (4) and (5) we see that they all have in common the nuclear g-factor. Thus we shall use the equations (32), (33), (34) to determine $g(I)$ in terms of experimentally observed A factors and calculated values of $\psi^2(r)$ and $\overline{r^2}$.

There is one other feature of line structure which calls for attention, as it is made use of in the experimental analysis. This concerns the relative intensities of the components of each line. The electric dipole moment \vec{P} of the extra-nuclear electrons satisfy a certain commutation rule with respect to the vectors \vec{J} , \vec{L} , and \vec{S} . In the notation of ref. (k), this is expressed in the form



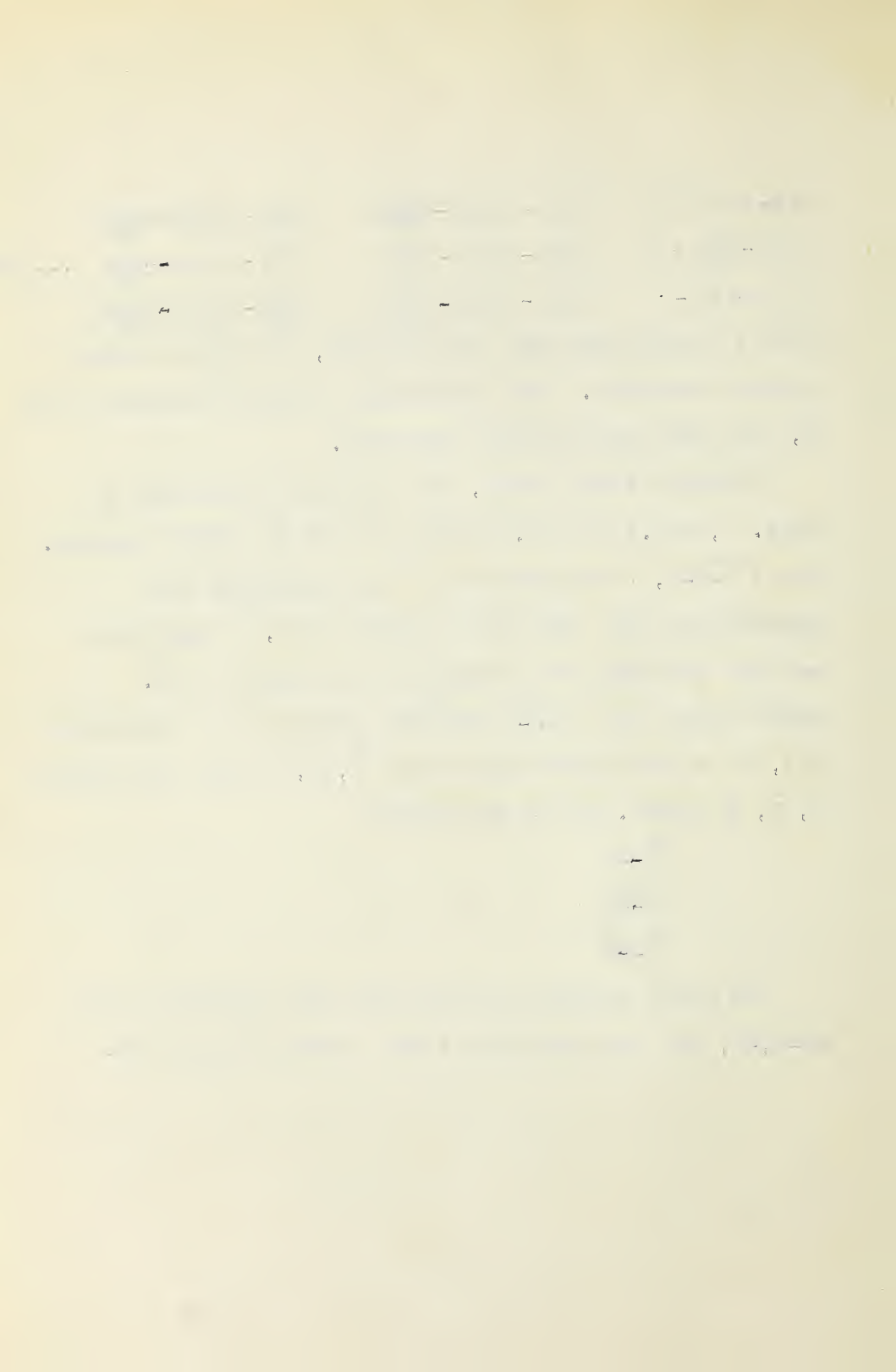
$$\begin{aligned}
 J_x P_x - P_x J_x &= 0 & J_x P_y - P_y J_x &= \frac{ihP_z}{2\pi} & J_x P_z - P_z J_x &= -\frac{ihP_y}{2\pi} \\
 J_y P_y - P_y J_y &= 0 & J_y P_z - P_z J_y &= \frac{ihP_x}{2\pi} & J_y P_x - P_x J_y &= -\frac{ihP_z}{2\pi} \dots (35) \\
 J_z P_z - P_z J_z &= 0 & J_z P_x - P_x J_z &= \frac{ihP_y}{2\pi} & J_z P_y - P_y J_z &= -\frac{ihP_x}{2\pi}
 \end{aligned}$$

with a similar set for the vector \vec{L} , the total orbital angular momentum. The third rule is that \vec{P} commutes with \vec{S} , the total spin angular momentum.

Through these rules, the intensity relations of chap. 9, sec.2 of ref.(k) are derived for (LS) coupling. Since $\vec{F} = \vec{J} + \vec{I}$, \vec{P} commutes with \vec{I} and satisfies the commutation rule (35) with respect to \vec{J} , it must also satisfy the analogous relation with respect to \vec{F} . Hence we may use these intensity relations of reference (k), if we correlate our vectors \vec{F} , \vec{J} , \vec{I} with the vectors \vec{J} , \vec{L} , \vec{S} of ref. (k) by the scheme

$$\begin{aligned}
 \vec{F} &\rightarrow \vec{J} \\
 \vec{J} &\rightarrow \vec{L} \\
 \vec{I} &\rightarrow \vec{S}
 \end{aligned}$$

We shall require in particular the selection rule $\Delta F = 0, \pm 1$, and the sum rule at the bottom of page 238.



APPARATUS AND EXPERIMENTAL PROCEDURE

A list of the essential apparatus and instruments used in this investigation together with a brief description of the function of each part is the following. A water-cooled hollow-cathode discharge

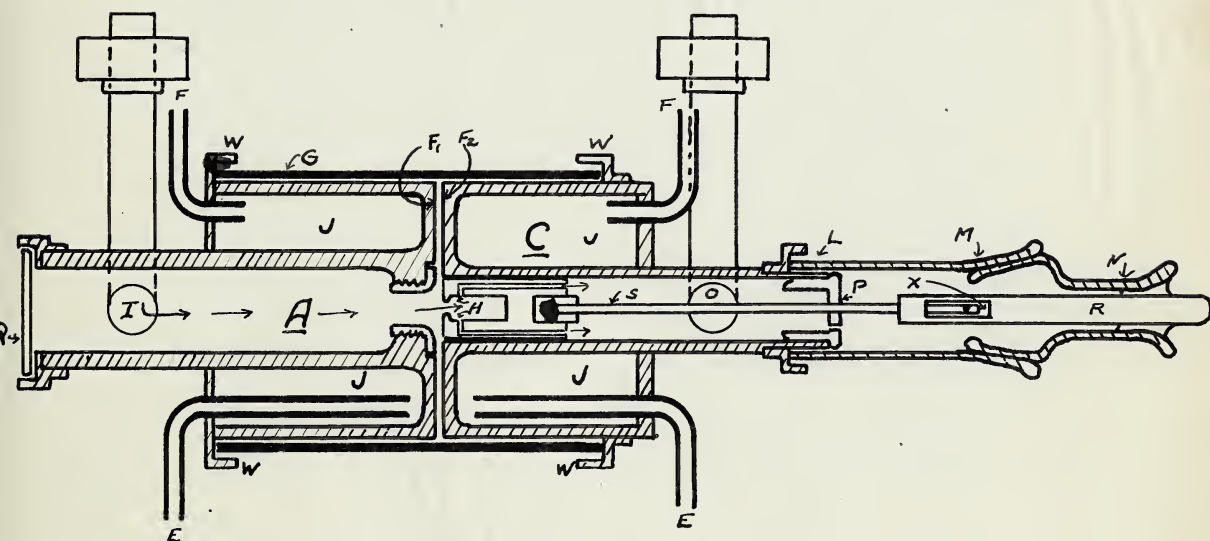


FIG. 1

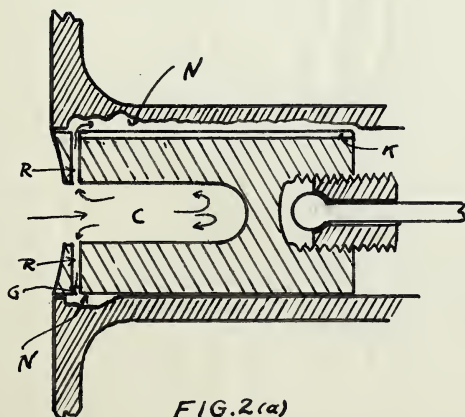


FIG. 2(a)

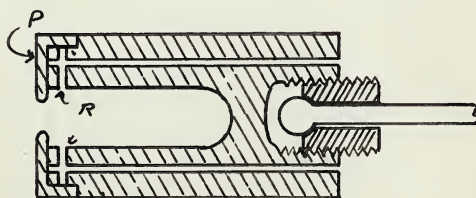


FIG. 2(b)

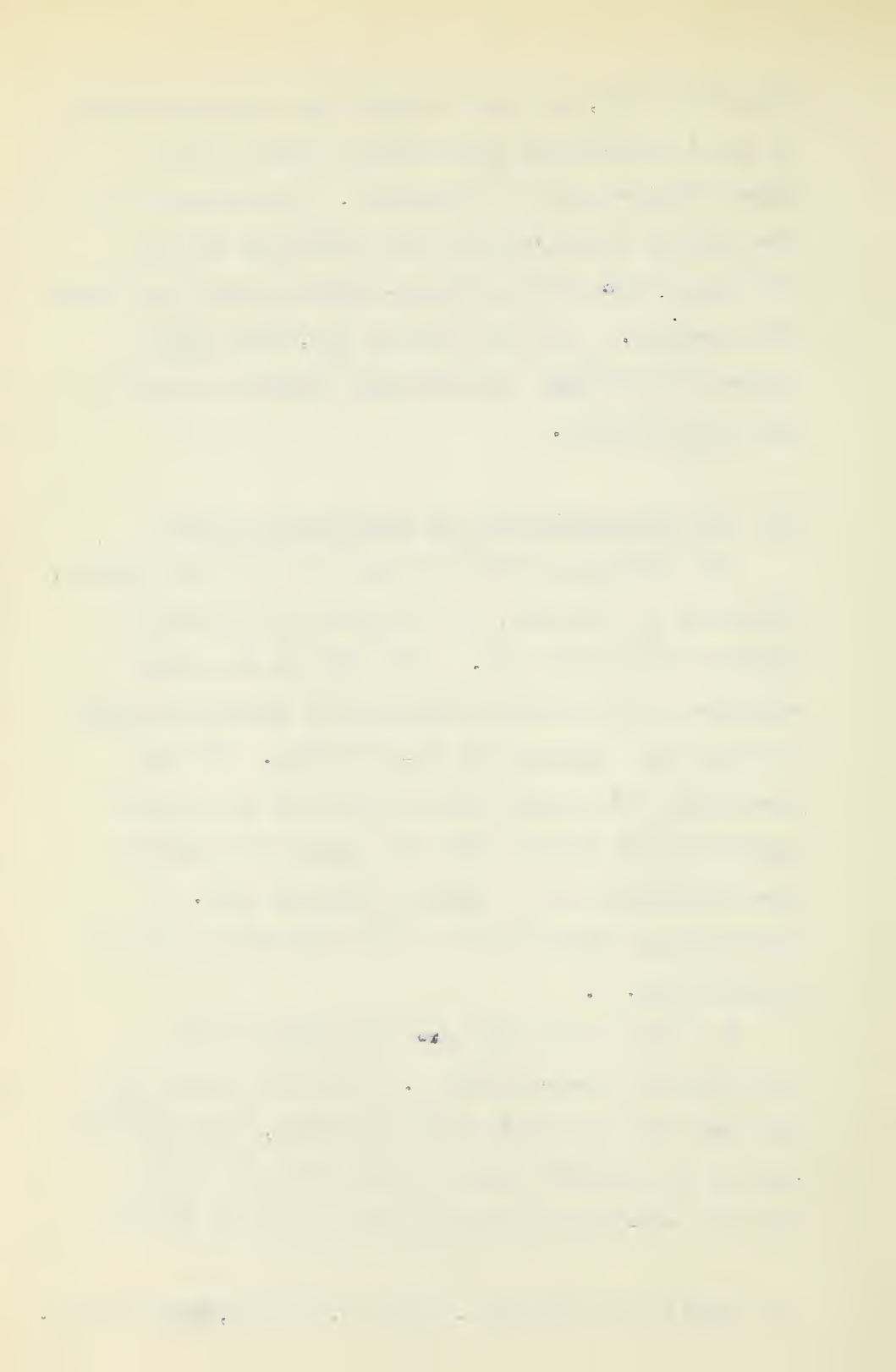
tube accompanied by a rare gas purification train was utilized to produce the spectrum of the thallium. Two crystal~~/~~line quartz and two glass Lummer - Gehrke plates were used individually to form interference fringes of the spectrum lines, thereby in general resolving each into its components. In the case of the bi-refrangent quartz plates, a Nicol or Wollaston prism was placed in the light beam immediately before the plates to eliminate one of the two plane-polarized components. The horizontal interference fringes so produced were focussed upon the slit of a Hilger E, spectrograph by means of a quartz-fluorite achromat rigidly attached to the spectrograph. The dispersed patterns of each spectrum line were then photographed together and the resultant photographic impressions measured by means of a Gaertner comparator reading to ~~xxxxx~~ 0.001 m.m. Subsequent calculations were performed mostly with the aid of an eight-figure Millionaire calculator. A more detailed description with diagrams of some of the above listed parts with a discussion of the associated experimental procedure follows. Section (A) deals with the light source and purification train, concluding with a digression on the candidate's unsuccessful attempt to further the analysis of the hyperfine structure of the gold spectrum.

In section (B), the theory underlying the measurement of small wave-number separations by use of the Lummer-Gehrke plate is discussed. A description of the optical arrangement of the apparatus and the necessary data for the Lummer-Gehrke plates concludes this section. The last section (C), deals with a number of pertinent experimental factors involved in the investigation.

(A) The Discharge Tube and Purification Train

The discharge tube was made up in the University, following in the main, the design of the lamp by Schüller and Gollnow (v). The body of the lamp consists of two separate cylindrical electrodes made of brass and sealed with Zn-Sn solder. The two electrodes fit loosely into either end of a pyrex cylinder which serves both the purpose of keeping them separated and of forming a vacuum seal. A longitudinal cross-section of the assembled lamp is shown in fig. 1.

A is the anode and C ~~is~~ the cathode with incorporated water-jackets J. These two parts were machined out of a solid brass cylinder, thus avoiding the use of soldered joints in the vicinity of the two flat end faces F_1 , F_2 which are likely to become



heated or acted upon by the discharge. These faces were separated a distance of about 1 m.m. by means of the glass cylinder G, the ends of which were ground square and flat, to insure proper alignment of the electrodes. Vacuum seals between the glass and electrodes were made at W with the aid of Dennis/on's Sealing Wax. The built-in water-jackets J serve both to control the temperature of the discharge taking place in the cavity H, and to prevent softening of the sealing wax. The inlets are at E and outlets at F. It was found unnecessary to electrically insulate the two cooling systems, if the lamp and water supply taps of the building were connected by about twenty feet of $\frac{1}{4}$ " rubber tubing. I and O are the inlet and outlet, respectively, for the rare gas. They are sealed to the purification train with sealing wax. The indicated direction of gas flow reduces diffusion of metallic vapor out of the cavity H and prevents it from condensing on the quartz window Q, which seals the anode and through which the light passes to the interferometer.

The cathode cavity H consists of a small solid aluminum cylinder. It slides into the central hollow cylinder of C with its front face coplanar with F_2 . Its other end is coupled with the head of a rod S which screws into a tapped plug P. P fits snugly

into C. A conical glass joint M is sealed to the cathode body at L. Into the glass plug N is sealed a hollow rod R with a long slot X. S slides into R and is fastened with a pin. Thus rotating the plug N translates the cavity H without danger of straining the ground joint, if H should become wedged.

The design of Schüler and Gollnow of the cavity was found unsatisfactory for the purpose of this investigation. This is shown in figure 2 (a). The incoming gas enters the cavity C (fig.2) and leaves it through six small radial channels R near the curved face F. The radial channels communicate with a peripheral groove G which is connected to the rear by the channel K along the cylinder. It was found that after several hours' run a discharge formed in the groove G. As brass sputters readily compared to aluminum, the body of the lamp disintegrated rapidly in the regions marked N, the intensity of disintegration increasing with the size of the cavity so formed. The result was the appearance of zinc and copper lines in the spectrum and a loss of control over the discharge. Further, the life of the lamp would have been very limited, for repairs at this point are impossible if the brass were burned through. The cavity shown in fig. 2 (b) was found to be more satisfactory. Again there are six radial channels but each is individually

connected to the rear by a longitudinal channel drilled through the aluminum cylinder. The cap P prevents ions from reaching brass at the ends of the radial channels and at the same time serves to retain the molten metal inside the cavity. It also restricts the diameter of the light source without limiting the volume of the cavity. This is a necessary feature when the Wollaston prism is in use as will be discussed under section (B).

In operation the discharge tube was sealed to the glass purification train shown diagrammatically in fig. 3. The system was filled with pure helium at a pressure of about 10 m.m. of mercury from the supply flask F. The two mercury diffusion pumps B, in series, circulate the gas in the direction of the arrows through the reservoir A, mercury trap C, into the liquid-air cooled activated charcoal trap D. This removes traces of any impurities in the helium except hydrogen. The purified helium then enters the lamp S at I, takes part in the discharge, and together with any other gases evolved, leaves through O to return to the pumps. The purpose of the reservoir A is to store up the helium after a run has been completed, so that it is not necessary to draw fresh gas from the supply F

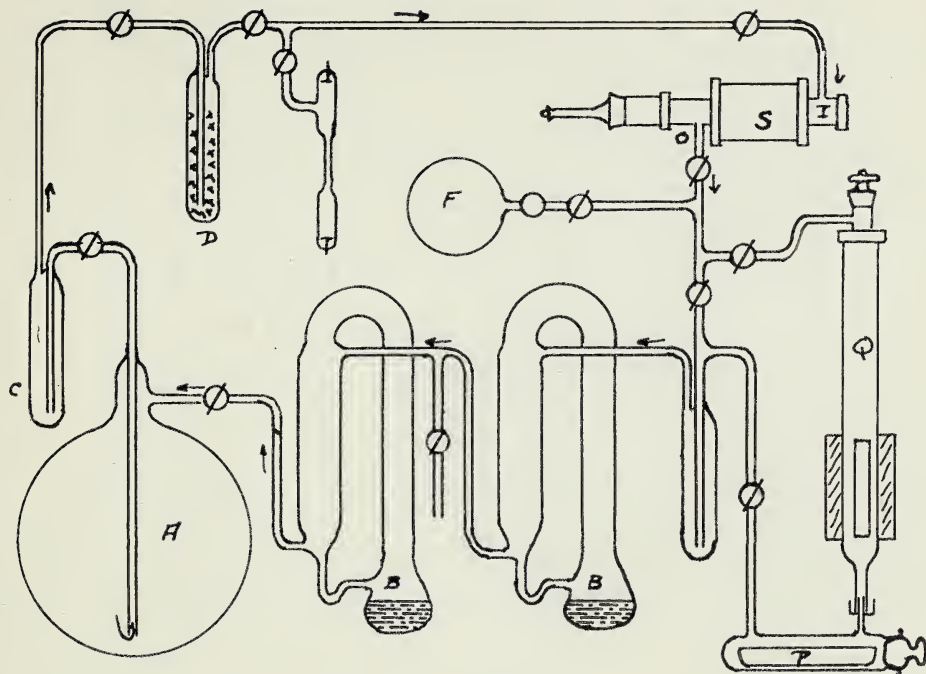


FIG. 3.

at the beginning of each run. The quartz tube Q is a cuprous-oxide hydrogen trap which together with the phosphorous pentoxide water-vapor trap P will remove hydrogen and water-vapor from the gas. This by-pass was also used to purify argon when it was tried in place of helium. Argon is absorbed in a charcoal trap such as D cooled with liquid air. By

passing the argon over successive boats in Q filled with calcium metal and cuprous oxide respectively, and heated to a temperature of about 700°C practically all chemically active gases were removed from it. Remaining impurities were finally removed in D cooled with carbon-dioxide snow.

During an exposure the discharge was operated at a pressure of about 10 m.m. Hg with a current of about 0.6 amperes. This resulted in a potential drop of about 300 volts across the lamp. The power was obtained from a full-wave rectified set consisting of two RCA - 872 mercury vapor valves; two 2000 volt 3KW transformers and a suitable filter. The current was controlled by a bank of four 1500 ohm water-cooled rheostats. It was found necessary to use this rather large current of 0.6 amperes in order to obtain photographs of the weak lines investigated in a reasonable exposure time. High temperature of the light source ensues large current with the resultant increased Doppler effect. However, a comparison of photographs with several taken with a lower current showed not appreciable broadening of the lines. With apparently constant conditions, the intensity of the Tl II lines varied considerably during an exposure, decreasing with a decreasing amount of thallium in the cavity. The thallium evaporated in the cavity,

condensed on the anode inset B (fig.1.) in a black powdery form, the deposit gradually building up to short-circuit the lamp. In order to increase available space for condensation, the inset was removed. Under these conditions exposures of more than fifty hours' duration could be obtained with about one gram of metal.

.

This is perhaps a suitable point at which to make a few observations concerning the candidate's efforts to obtain measurements in the hyperfine structure of the gold spectrum. A few lines of the Au I spectrum have been resolved and measured by previous investigators (y), and an attempt was made to further the measurements in the spectra of both Au I and Au II.

Original trials to excite an intense spectrum were made with a different type of discharge tube. It consisted of a large brass anode cylinder externally water-cooled, with a small uncooled cathode suspended at its center. Iron, carbon and Molybdenum cathodes of various shapes and sizes were tried. At a temperature below the melting point of gold, iron sputtered more readily, covering the gold with ~~an~~ a film. Above its melting point, an iron-gold alloy was formed with the loss of both

(y) Ritschl - Naturwissenschaften², 690, (1931).
Wolff- Phys.Rev.44,512, (1933)

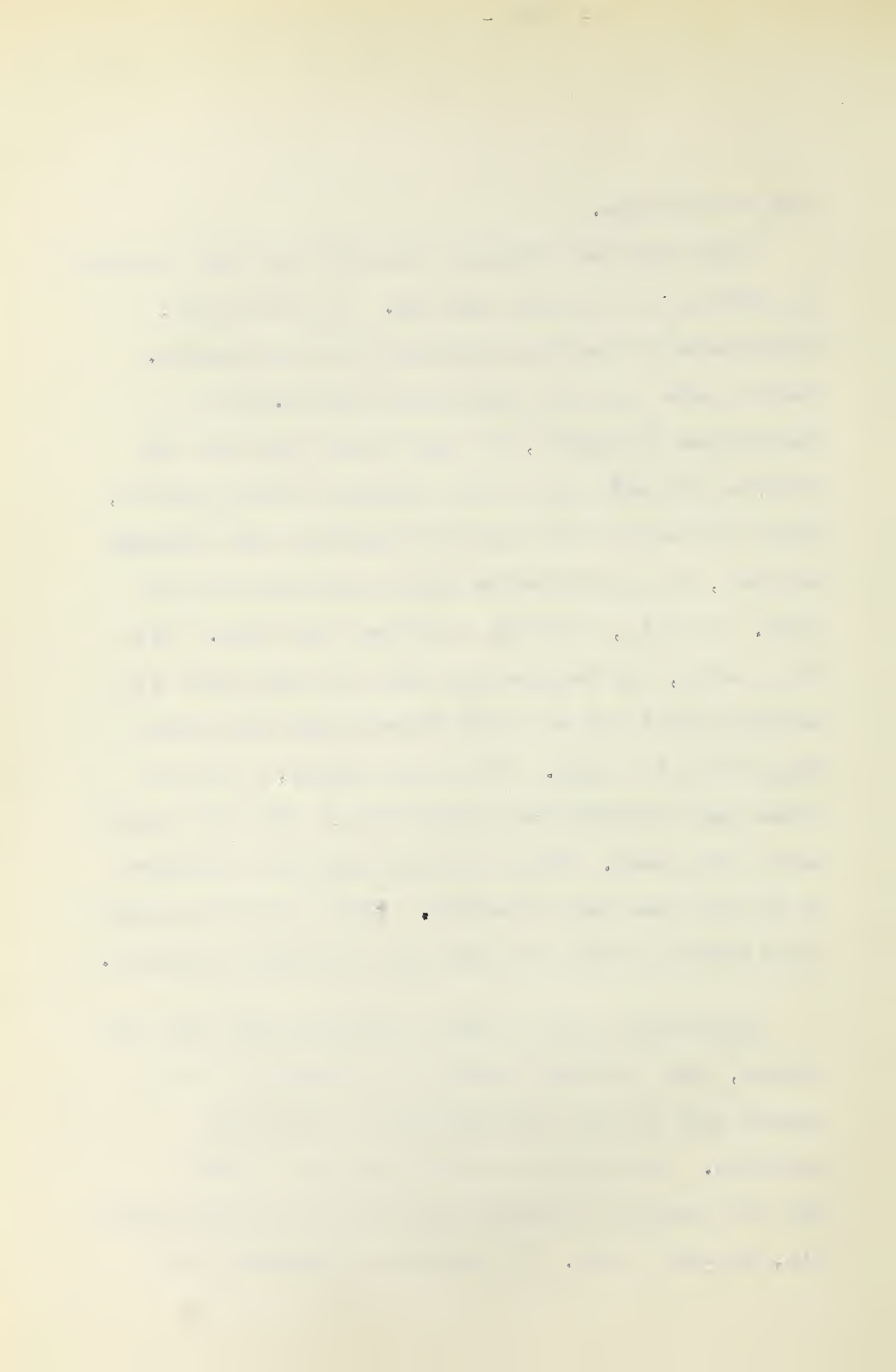
spectrum and gold. The carbon electrodes were better in this respect, but when the gold melted it rolled up into a ball, thereby lessening the chances of getting a strong spectrum. Further, the carbon electrodes continually poured out impurities in the discharge thereby producing a rich band spectrum which obliterated any existing gold lines. Baking the electrode in a vacuum at red heat for many hours before introducing it into the lamp did not greatly improve the situation. A sheet molybdenum cathode of small dimensions seemed to be about the best. But since many molybdenum lines as well as bands made their appearance, it was impossible even with this to obtain a spectrum free of doubtful lines.

Under the best conditions of excitation, the gold was in a molten state, thus evaporating freely and condensing on the window of the lamp through which the light passed. This made it necessary to open the lamp frequently. After a few hours' run, a thin film of metal condensed on the anode surface. When the lamp was opened and exposed to air, days were required to diminish the flow of gases coming

out of the film.

This lamp was finally discarded and that designed by Schüler and Gollnow made up. In this lamp, molybdenum and carbon cathodes were tried again. Carbon gave the same trouble as before. With a molybdenum electrode, the gold never covered the surface properly due to the cathode cooling system, with the result that the Mo I spectrum was strongly excited, the sputtered Mo ions condensing on the gold. Finally, aluminum cathodes were made. With this metal, the temperature must be kept below its melting point and one must depend upon sputtering only for gold vapor. With pure helium, a fairly clean Au I spectrum was obtained but this was in all cases very weak. Only enticing momentary glimpses of Au II lines were obtained, these appearing under conditions in which the lamp was extremely unstable.

According to the data of Blechschmidt (aa) and others, gold sputters readily as compared to the metals used in the construction of the hollow cathodes. Of course, his data does not include the low range of voltages used in this investigation viz. 200-600 volts. On examining Blechschmidt's

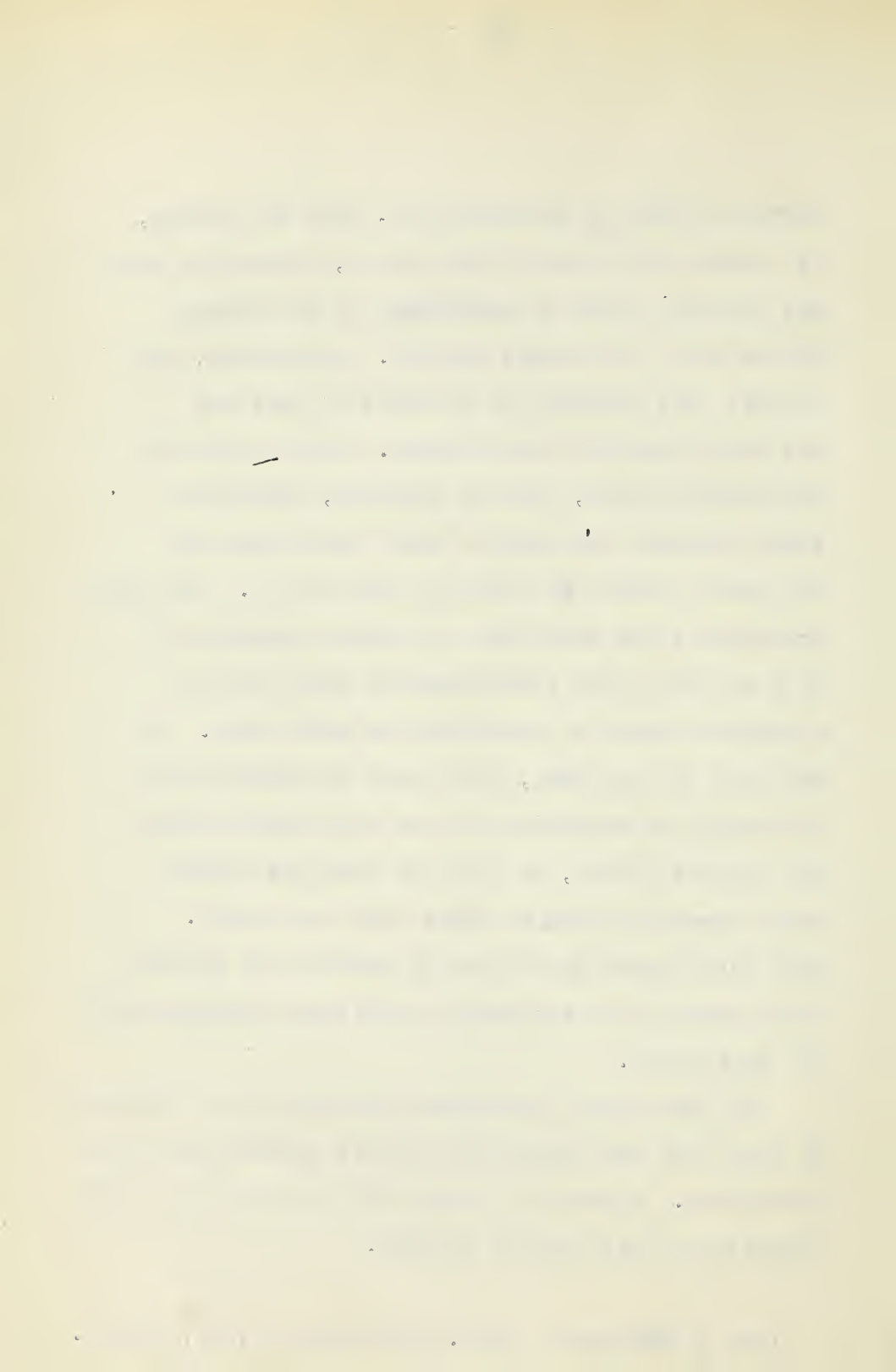


curves of rate of sputtering vs. applied voltage, it appears that some of them cross, indicating that the relative rates of sputtering of two metals varies with the voltage applied. Apparently, this is what has happened in the case of gold and the metals used in the cathodes. With a metal of low melting point, such as thallium, sputtered atoms probably form only a small percentage of the vapor formed by ordinary evaporation. The best arrangement for obtaining an intense spectrum of Au I and Au II for interferometer work would be a separate means of producing the gold vapor. In the kind of lamp used, this might be accomplished by placing an evaporator in the anode just before the cathode cavity, so that the rare gas stream would sweep the metallic vapor into the cavity. This arrangement would make it possible to control vapor density and excitation conditions independently of each other.

The excitation processes occurring in a discharge of this kind are complicated and at present not fully understood. A paper by Sawyer (bb) is about the most complete on this subject to date.

(aa) Blechschmidt - Ann. der Physik 81,999, (1926).

(bb) Sawyer - Phys.Rev. 36,44, (1930).



(B) Theory of Lummer - Gehrke Plate

The Lummer-Gehrke plate consists of a long rectangular glass or quartz plate with two optically plane and parallel faces, to one end of which is cemented a prism. A cross-section perpendicular to the plane of the optical faces is shown in fig.4, in which PQ and RS are the optical faces, and SXY the prism.

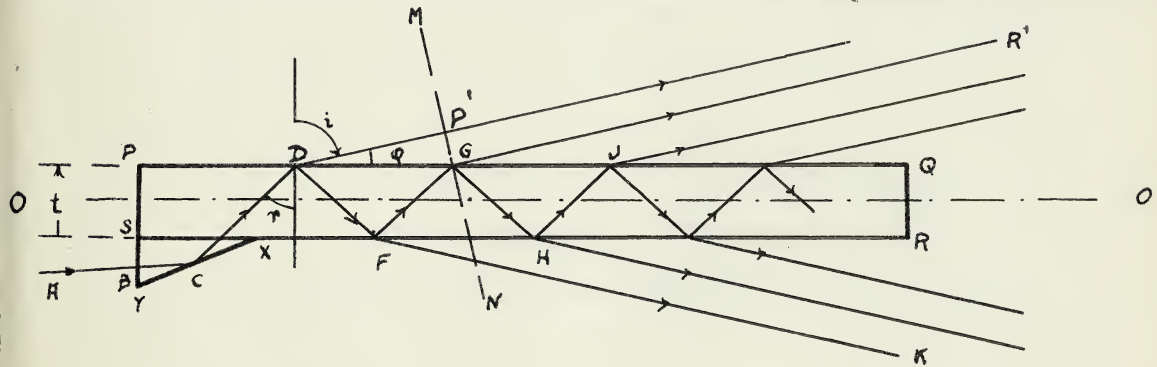


FIG. 4.

Let us consider a ray of light of wave-length λ incident upon the base of the prism at B. It is totally reflected at C to D where it is partially transmitted along DP' and partially reflected along DF . At F it is again divided into a reflected ray FG and transmitted ray FK . The same process is repeated at the points G, H, J, etc. Thus to each ray entering the prism at B, there is a system of parallel

rays emerging from the face PQ and another system emerging from the face SR, these two systems being symmetrically directed about the axis O. Consider any plane MN which is perpendicular to the direction of the rays DP', GR', etc. If all the rays belonging to this system reach the plane in phase, a line of maximum illumination perpendicular to the plane of the paper will be formed, in the focal plane of the lens L through which they pass. If on the other hand alternate rays of the system reach the plane MN differing in phase by an odd multiple of π , they will nearly annul each other, with a resultant line of minimum illumination in the focal plane of the lens. The annulment will not be complete since consecutive rays are not of equal amplitudes. Thus, as the angle of emergence i of the rays is changed, there will be a succession of parallel bright and dark fringes formed in the focal plane of the lens. A ray of different wave-length will form a different set of such fringes. If the difference in wave-length is small, it is possible to determine its magnitude by a measurement of the two sets of fringes. It is the object of this section to indicate how this is performed. Referring to fig.4, let

- t - thickness of the plate.
- μ - index of refraction of the plate with respect to air.
- r - angle of incidence of ray CD to normal at D.
- i - angle of emergence of ray DP' at D.
- ϕ - the grazing angle at D.

The optical path difference of the ray GR' and DP' at the plane MN through G is

$$\delta = \mu(\overline{DF} + \overline{FG}) - \overline{DP'}$$

This is readily reduced to the form

$$\delta = 2t.\mu.\cos(r) \dots\dots\dots(1)$$

If this system of rays is to produce a line of maximum illumination, then we must have

$$\delta = n\lambda = 2t.\mu.\cos(r) \dots\dots\dots(2)$$

where n is a positive integer.

By application of Snell's Law of refraction this reduces to

$$\delta = n\lambda = 2t\sqrt{\mu^2 - \sin^2 i} \dots\dots\dots(2')$$

This equation states that the bright fringe of order n of the wave-length λ is formed by the light emerging from the plate at an angle i.

Since n is large, we can determine the difference in the angles of emergence $(\delta i)_\lambda$ of the orders n and n+1 for wave-length λ by differentiating and setting

$\delta n = 1$. After rearranging the terms we have

$$(\delta i)_\lambda = \frac{-n\lambda^2}{4t^2 \sin i \cos i} = - \frac{\lambda \sqrt{\mu^2 - \sin^2 i}}{2t \sin i \cos i} \dots\dots\dots(3)$$

where n λ is replaced by its value from (2').

Suppose now that the beam of light incident upon the prism at B is not monochromatic but composed of two wave-lengths λ and $\lambda + \delta\lambda$. Then the angular separation $(\delta i)_n$ of the fringes of λ and $\lambda + \delta\lambda$ for the same order n is obtained by differentiating with n constant. After simplification we obtain

$$(\delta i)_n = - \left(\frac{n^2 \lambda}{4t^2} - \mu \frac{\partial \mu}{\partial \lambda} \right) \cdot \frac{\delta \lambda}{\sin i \cos i} \dots\dots\dots(4)$$

If $(\delta i)_n = (\delta i)_\lambda$, then the fringe of order n for wave-length $\lambda + \delta\lambda$ just coincides with the fringe of order $n+1$ for wave-length λ . Hence, setting (3) equal to (4) will enable us to determine this wave-length difference, which will be denoted by $\Delta\lambda$. We have then

$$\begin{aligned} \frac{-\lambda \sqrt{\mu^2 - \sin^2 i}}{2t \sin i \cos i} &= -\left(\frac{n^2 \lambda}{4t^2} - \mu \frac{\partial \mu}{\partial \lambda}\right) \cdot \frac{\Delta\lambda}{\sin i \cos i} \dots\dots\dots (5) \\ -\frac{\lambda \sqrt{\mu^2 - \sin^2 i}}{2t} &= -\lambda \left(\frac{n^2 \lambda^2}{4t^2} - \mu \lambda \frac{\partial \mu}{\partial \lambda}\right) \cdot \Delta\lambda \\ &= -\frac{1}{\lambda} (\mu^2 - \sin^2 i - \mu \lambda \frac{\partial \mu}{\partial \lambda}) \Delta\lambda \quad \text{by (2')} \\ \therefore \frac{\Delta\lambda}{\lambda^2} &= \frac{\sqrt{\mu^2 - \sin^2 i}}{2t (\mu^2 - \sin^2 i - \mu \lambda \frac{\partial \mu}{\partial \lambda})} \end{aligned}$$

Now, i is nearly $\frac{\pi}{2}$ for the fringes considered and the above relation has been found to be sufficiently accurate if we set $\sin^2 i = 1$. We also introduce the wave-number $\nu = \frac{1}{\lambda}$ and replace $\frac{\Delta\lambda}{\lambda^2}$ by $-\Delta\nu$.

Hence the above expression becomes

$$\Delta\nu = \frac{-\sqrt{\mu^2 - 1}}{2t (\mu^2 - 1 - \mu \lambda \frac{\partial \mu}{\partial \lambda})} \dots\dots\dots (6)$$

where $\Delta\nu$ is the wave-number difference between the two components such that the fringe of order n of the smaller ν just coincides with the fringe of order $n+1$ of the greater ν .

The expression tells us that if we have two fringes of the same order near each other, that one corresponding to the smaller angle ϕ (fig.4) has the greater ν . The $\Delta\nu$ for a given wave-length may be evaluated from a knowledge of the optical constants of the plate, and will be dealt with more fully later.

The method of determining $\delta\lambda$ or $\delta\nu$ of two components is due to McLennan and McLeod (w).

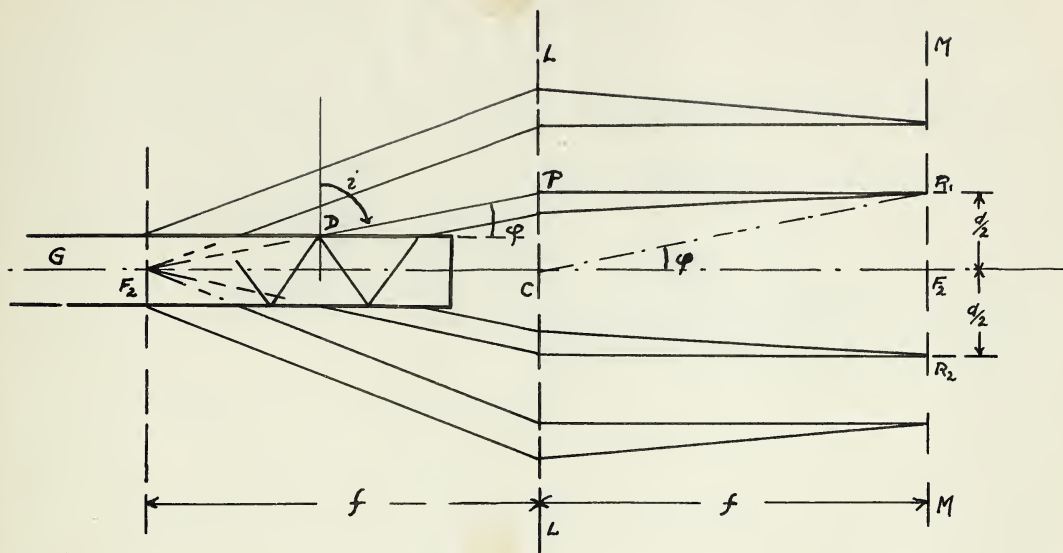


FIG. 5.

The experimental arrangement is to allow the light emerging from both sides of the Lummer plate G to pass through the lens whose principal plane is represented by LL^(Fig. 5). The lens brings it to a focus in its focal plane MM. (each system of rays such as represented in fig. 4 is a parallel beam brought to a line focus in the focal plane of the lens). If the plane MM coincides with the slit of a stigmatic spectrograph, then a section of the interference fringes may be photographed and subsequently measured.

It is impossible to measure the angles i or φ directly but one can measure the distance d between fringes of the same order on opposite sides of the center F₂. By selecting from any parallel beam

a ray DP which when produced backwards will pass through the focal point F , it is obvious that the angle FCR , is equal to ϕ where C is the center of the projecting lens and R , is the point at which that beam comes to a focus.

$\therefore \tan \phi = \frac{d_n}{2f}$ where f is the focal length of the lens; d_n is the distance between fringes of the same order n on opposite sides of the center i.e. $d = \overline{RR'}$

Since ϕ is small we put

$$\tan \phi \sim \sin \phi \sim \frac{d_n}{2f}$$

Substituting this in (2') we obtain

$$n\lambda = 2t \sqrt{\mu^2 - 1 + \frac{d_n^2}{4f^2}} \quad \dots\dots\dots (7')$$

Or, upon squaring

$$\frac{n^2 \lambda^2}{4t^2} = \mu^2 - 1 + \frac{d_n^2}{4f^2} \quad \dots\dots\dots (7)$$

The difference between the fringes of order n and $n+1$ for wave-length λ is given in terms of the difference $d_{n+1}^2 - d_n^2$ by differentiating and setting $\delta n = 1$ as before.

We obtain

$$2 \frac{n\lambda^2}{4t^2} = \frac{d_{n+1}^2 - d_n^2}{4f^2} \quad \dots\dots\dots (8)$$

Similarly, we obtain the difference $\delta \lambda$ in terms of the difference $d_n'^2 - d_n^2$ where d_n' is the distance d for $\lambda + \delta \lambda$ of order n .

We have $\frac{n^2 \lambda^2}{4t^2} \delta \lambda = 2\mu \frac{\partial \mu}{\partial \lambda} \delta \lambda + \frac{d_n'^2 - d_n^2}{4f^2}$

or $2 \left(\frac{n^2 \lambda^2}{4t^2} - \mu \lambda \frac{\partial \mu}{\partial \lambda} \right) \frac{\delta \lambda}{\lambda} = \frac{d_n'^2 - d_n^2}{4f^2}$

Using (2') this becomes

$$2 \left(\mu^2 - \sin^2 i - \mu \lambda \frac{\partial \mu}{\partial \lambda} \right) \frac{\delta \lambda}{\lambda} = \frac{d_n'^2 - d_n^2}{4f^2} \quad \dots\dots\dots (9)$$

Replacing $\frac{\delta\lambda}{\lambda^2}$ by $-\delta\nu$, $\sin^2 i$ by 1, and rearranging, we get

$$\delta\nu = -\frac{1}{\lambda} \frac{1}{2(\mu^2 - 1 - \mu\lambda \frac{\partial\mu}{\partial\lambda})} \cdot \frac{d_n'^2 - d_n^2}{4f^2}$$

Using (8) to eliminate the factor $\frac{1}{4f^2}$, we have

$$\begin{aligned} \delta\nu &= -\frac{1}{2\lambda} \frac{1}{(\mu^2 - 1 - \mu\lambda \frac{\partial\mu}{\partial\lambda})} \cdot \frac{2n\lambda^2}{4f^2} \cdot \frac{d_n'^2 - d_n^2}{d_{n+1}' - d_n^2} \\ &= -\frac{\sqrt{\mu^2 - 1}}{2t(\mu^2 - 1 - \mu\lambda \frac{\partial\mu}{\partial\lambda})} \cdot \frac{d_n'^2 - d_n^2}{d_{n+1}' - d_n^2} \\ &= \Delta\nu \cdot \frac{d_n'^2 - d_n^2}{d_{n+1}' - d_n^2} \quad \text{by eqn (6)} \quad \dots\dots\dots (10) \end{aligned}$$

Hence, $\delta\nu$ can be determined in terms of the calculated $\Delta\nu$ and the measured values d .

However, it very often happens that the n 'th order of one component does not lie between the n 'th and $n+1$ 'th orders of the other. If this is not the case then it is necessary to add $\Delta\nu$'s to the expression (10) equal in number to the number of fringes overlapped. Thus it is easy to see that results derived from one plate are not unambiguous. But, if a pattern for the same spectrum line is obtained with a plate of different optical properties, the amount of overlap as well as the fractional part (10) will in general be different. The method of obtaining an unambiguous result for the separation of two components is then to measure two patterns obtained with different plates, and adding to the fractional parts (10) of each, the corresponding $\Delta\nu$'s until a coincidence in value is obtained.

As was mentioned above, the Δn for each plate are calculated from a knowledge of its optical constants. For the particular plates used, the following is a list of the details.

1. One quartz plate of length 13 cm. and thickness 0.4493 cm. with optic axis parallel to the long edge. The extraordinary ray was eliminated and a dispersion formula due to Coode-Adams (x) was used to calculate and μ in the range $\lambda 2600 - \lambda 3000 \text{ \AA}$. The calculated values of μ agreed to one unit in the fifth decimal place with experimental values.
2. One quartz plate of length 13 cm. and thickness 0.5825 cm. with the optic axis parallel to the short edge of the reflecting face of the plate. The ordinary ray was eliminated and a single three term Cauchy formula was used in the range $\lambda 2600 - \lambda 3000 \text{ \AA}$. The calculated values of μ agreed to one unit and better in the fifth decimal place.
3. Two glass plates, one of length 13 cm. and thickness 0.4872 cm.; the other of length 20 cm. and thickness 0.6198 cm. Cauchy formulae were used in both cases in the range $\lambda 6110 - \lambda 6180 \text{ \AA}$ but there were only sufficient experimental values of μ to determine the constants of the formula.

The optical arrangement of the apparatus was as follows.

(x) Coode - Adams.- Proc. Roy. Soc. A 117, 209, (1927)

The light from the discharge tube passed through a small aperture five-inch quartz lens placed immediately in front of the lamp. The condensed beam passed through a second quartz lens of focal length six inches, which formed an image of the light source on the prism base of the Lummer plate. The size of the image as well as the cross-section of the light beam between these two lenses was governed by the mutual distances between the lenses and light source. With this arrangement of lenses, the maximum of light incident on the Lummer plate was used in the formation of fringes of low order, from which best measurements are obtainable. After passing through the Lummer plate, mounted on an adjustable holder, the light was brought to a focus on the spectrograph slit by means of an achromatic lens of focal length 23 cm.

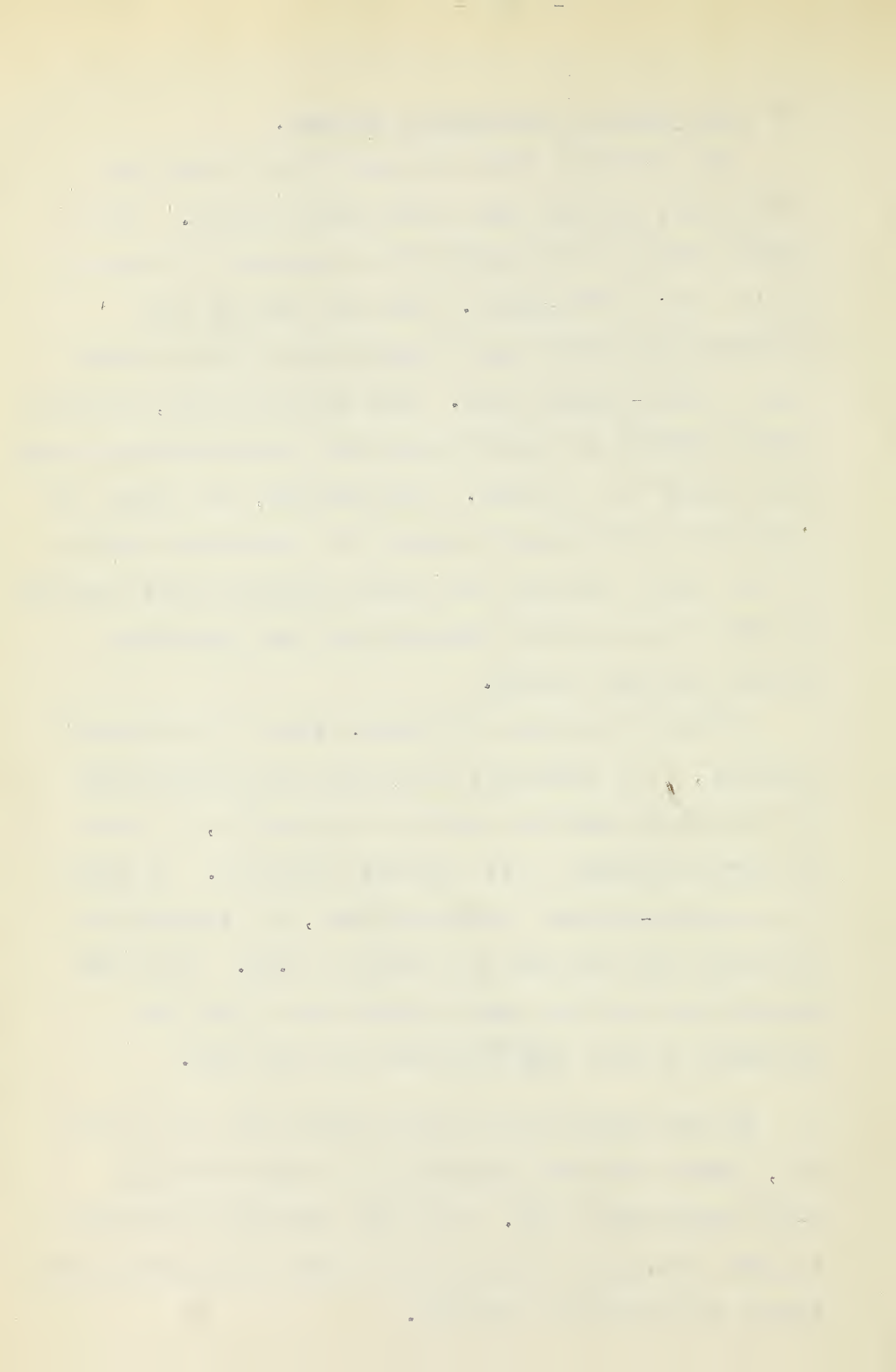
As was discussed under INTRODUCTION, a Wollaston prism was used for the region 2600 - 3250Å to separate the component light vibrations before allowing one to pass through the Lummer plate. A small diameter light source, sharply defined, was of great advantage in separating them.

(C) Some General Experimental Factors.

The discharge tube and purification train were permanently mounted upon an adjustable table. The Lummer plate and its holder were enclosed in a double-walled box of "Ten-Test". Both the box and the spectrograph rested upon a rigid steel girder mounted upon a stone-topped bench. With this mounting, relative motion between the spectrograph and interferometer system was reduced to a minimum. Nevertheless, the effect of mechanical vibrations, due mainly to pedestrian traffic in the nearby corridor and lecture room, was quite evident on most of the plates obtained from long exposures running through the day.

During an exposure of greater than a few minutes' duration, it is essential to maintain the temperature of the Lummer plate as constant as possible, in order to prevent changes in its optical constants. By means of a mercury-contact thermoregulator, the temperature variation was confined to a range of 0.4°C . The room temperature was also under control but it was not necessary to have the ^{same} precision in this case.

In the ultra-violet region Eastman 33; and in the red, Eastman Process Panchromatic and Spectroscopic S-III plates were used. They were generally developed in Agfa fine-grain developer and fixed in an acetic-acid fixing and hardening solution.



EXPERIMENTAL RESULTS AND DISCUSSION

The lines analyzed together with the hyperfine splittings of their initial levels are presented below. For each line, the approximate wave-length in Å units is given at the top left; with its classification, as taken from the tables of Ellis and Sawyer (g), immediately to the right. At the top right is given the separation of the final level $\Delta(n^2 L_j)$ in wave-number units (cm^{-1}) and the reference from which it was obtained. We recall that

(i) - Schuler and Keyston - Zeit.f. Physik 70,1,(1931).

(j) - Smith and Convey - Can.Journ. of Research A14,133(1936)

The diagram at the left represents the initial and final levels of the line investigated; the labels to the right of each level, its f value. The hyperfine separations are drawn approximately to scale, but the separation between J levels are not. The vertical arrows in each diagram, with the labels A, B, C, etc. represent the components of the line which were observed and interpreted as belonging to the indicated levels. The numbers near these are the theoretically expected relative intensities. The wave number separations of these components are given in the table to the right. In this table, the symbols Q6, Q4 signify that the

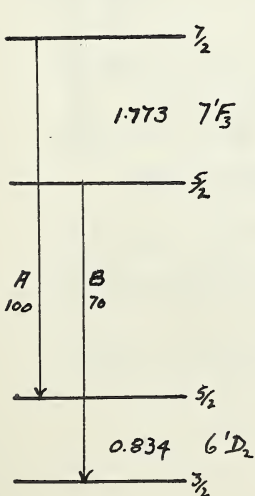
measurement to the right of them were obtained from the quartz Lummer plate of thickness 5.825 mm., and 4.872 mm. respectively. Generally, if one of these symbols is repeated in a table, two different photographs have been measured. If the symbol Q4_{pr6} is followed by (blend), the components have not been resolved on that plate and the measurement to the right has been disregarded in obtaining the average.

The interpretation of the structure of the lines in the red region, belonging to the 6s⁵F-6s6g multiplet has not been completed. Sufficient measurements are at hand, but the patterns are so complex, that the interpretation was found difficult.

.....

λ 2703...6 'D₂-7 'F₃

Δ (6 'D₂) = 0.834 (i)



<u>Plate</u>	<u>(A-B)</u>
Q6	0.931
Q6	0.940
Q4	0.921
Q6	0.945
Av.	0.939 ± 0.005

$\therefore \Delta$ (7 'F₃) = 1.773

Handwritten text, mostly illegible due to fading. Some words like "The" and "and" are visible.

Handwritten text, possibly a date or a short phrase.

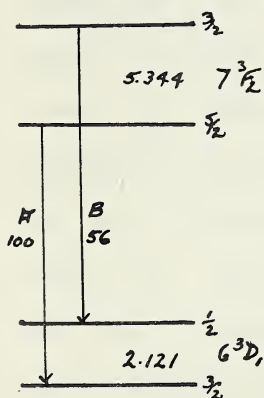
Large block of handwritten text, mostly illegible. Some words like "The" and "and" are visible.

Smith and Convey (j) give a value of 0.695 for (7^1F_3) through an interpretation of the line $\lambda 4286$. However, on checking this result it was found to be 1.809. The difference between these two values is probably due to the fact that the separation of the final level of $6p^3P_1$ of $\lambda 4286$ is unreliable as may be seen by examining the table in their paper. Also, the value obtained by them is derived from only one measurement.

.....

$\lambda 2780 \quad 6^3D_1 - 7^3F_2$

$\Delta(6^3D_1) = -2.121 \text{ (i)}$



<u>Plate</u>	<u>B - A</u>
Q6	3.225
Q6	3.223
Q4(blend)	3.223
Av.	<u>3.224 ± .001</u>

$\therefore \Delta(7^3F_2) = -5.344$

This line was resolved on a photograph of the ordinary line spectrum. A measurement of the separations on the line spectrum agreed as well as could be expected with the above result.

.....

$\lambda 2801 \quad 6^3D_2 - 7^3F_{2,3}$

$$\Delta(6^3D_2) = 0.555 \text{ (i)}$$

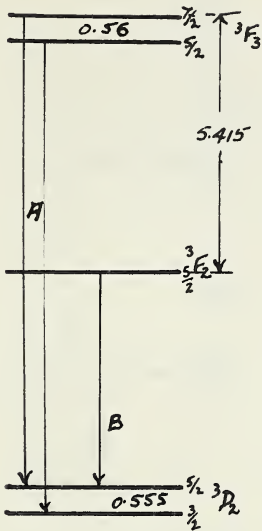


Plate	A - B
Q6	5.419
Q6	5.409
Q4	5.420
<u>Q4</u>	<u>5.414</u>
Av.	5.415 \pm .003

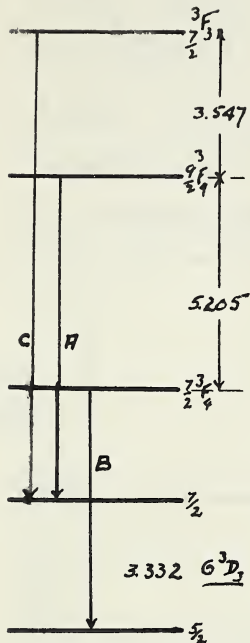
$$\therefore \Delta(7^3F_3) = 0.56$$

$$\frac{3}{2}F_3 - \frac{3}{2}F_2 = 5.415$$

In this line two components A and B were observed. The component A was much more intense than B so that these two could not both be from the level 3F_3 . Hence it was inferred that A was a superposition of the two components from the level 3F_3 and B the strongest expected component from the level 3F_2 . The line $\lambda 2801$ was again resolved on the line spectrum, so that a rough check of the above values for A - B was possible.

.....

$\lambda 2833 \quad 6^3D_3 - 7^3F_{3,4}$



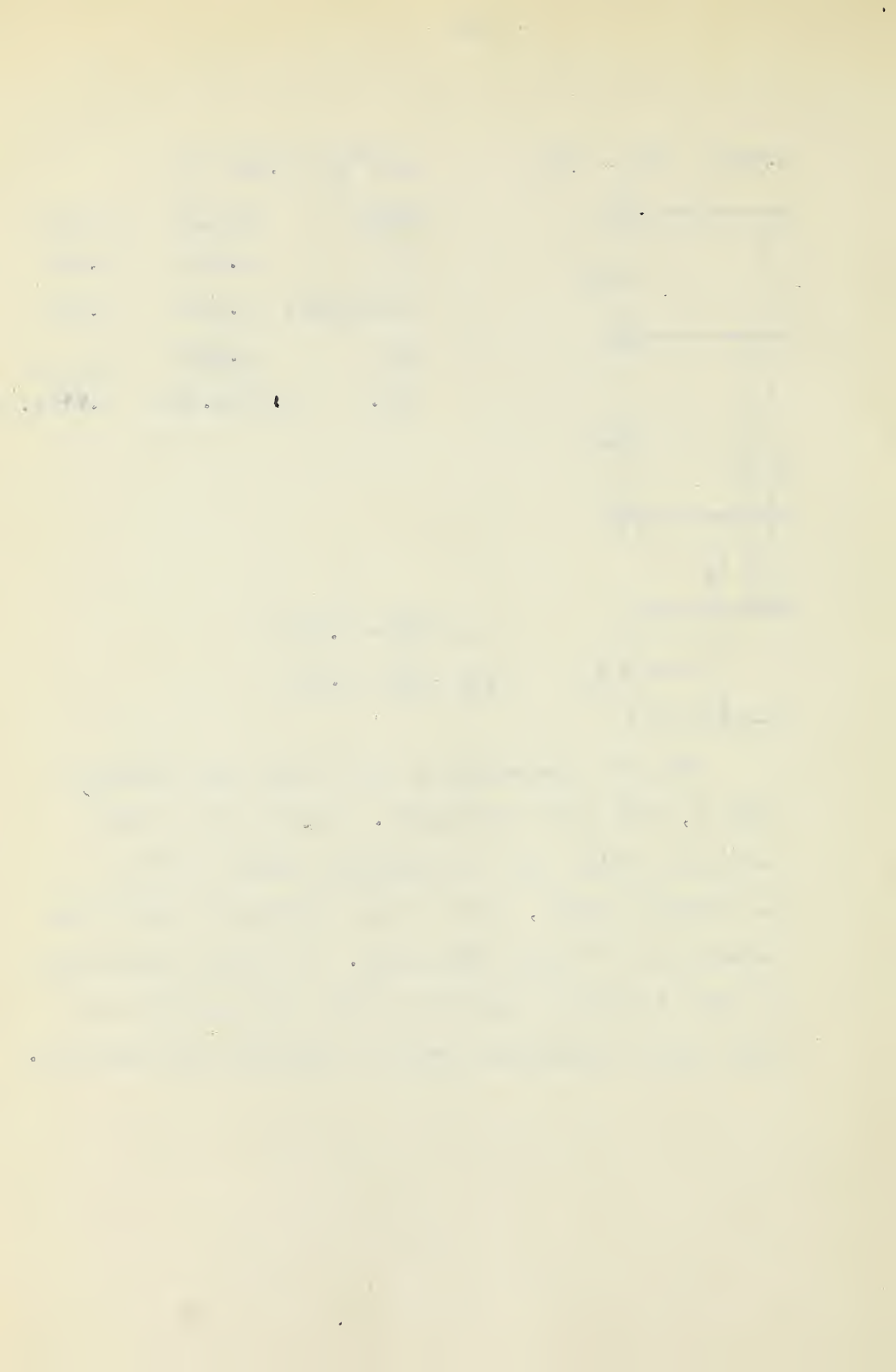
$$\Delta(6^3D_3) = 3.332 \text{ (j)}$$

Plate	A - B	C - A
Q4	1.878	3.530
Q6(blend)	1.852	3.565
<u>Q4</u>	<u>1.869</u>	<u> </u>
Av.	1.873 \pm .005	3.547 \pm .018

$$\Delta(7^3F_4) = 5.205$$

$$\frac{3}{2}F_3 - \frac{3}{2}F_4 = 3.547$$

Both the components A and B were much stronger than C, with A the strongest. Hence A and B were taken as having the two hyperfine levels of 3F_4 as initial levels, and C as the strongest transition between the 3F_3 and 6^3D_3 levels. The three components of this line were resolved on the line spectrum and thus their separations could be checked approximately.



Combining the results of the lines $\lambda 2780$, $\lambda 2801$, $\lambda 2833$, completes the analysis of the fine and hyperfine structure of the 7^3F term. A diagram is shown in fig.8. To the ~~right~~^{left} of the diagram, all those separations obtained from each line are bracketed.

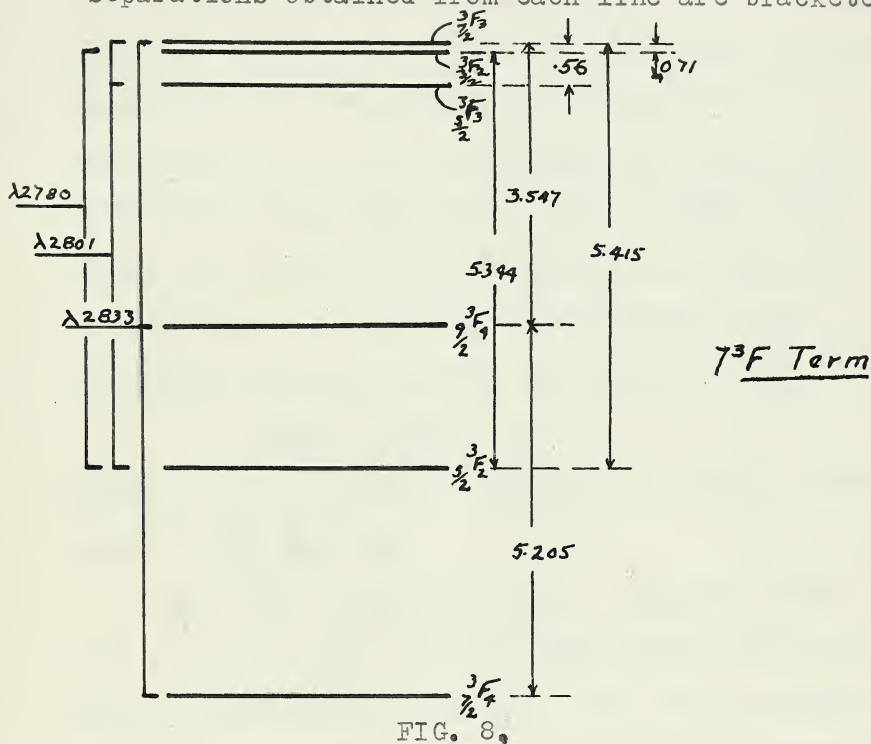
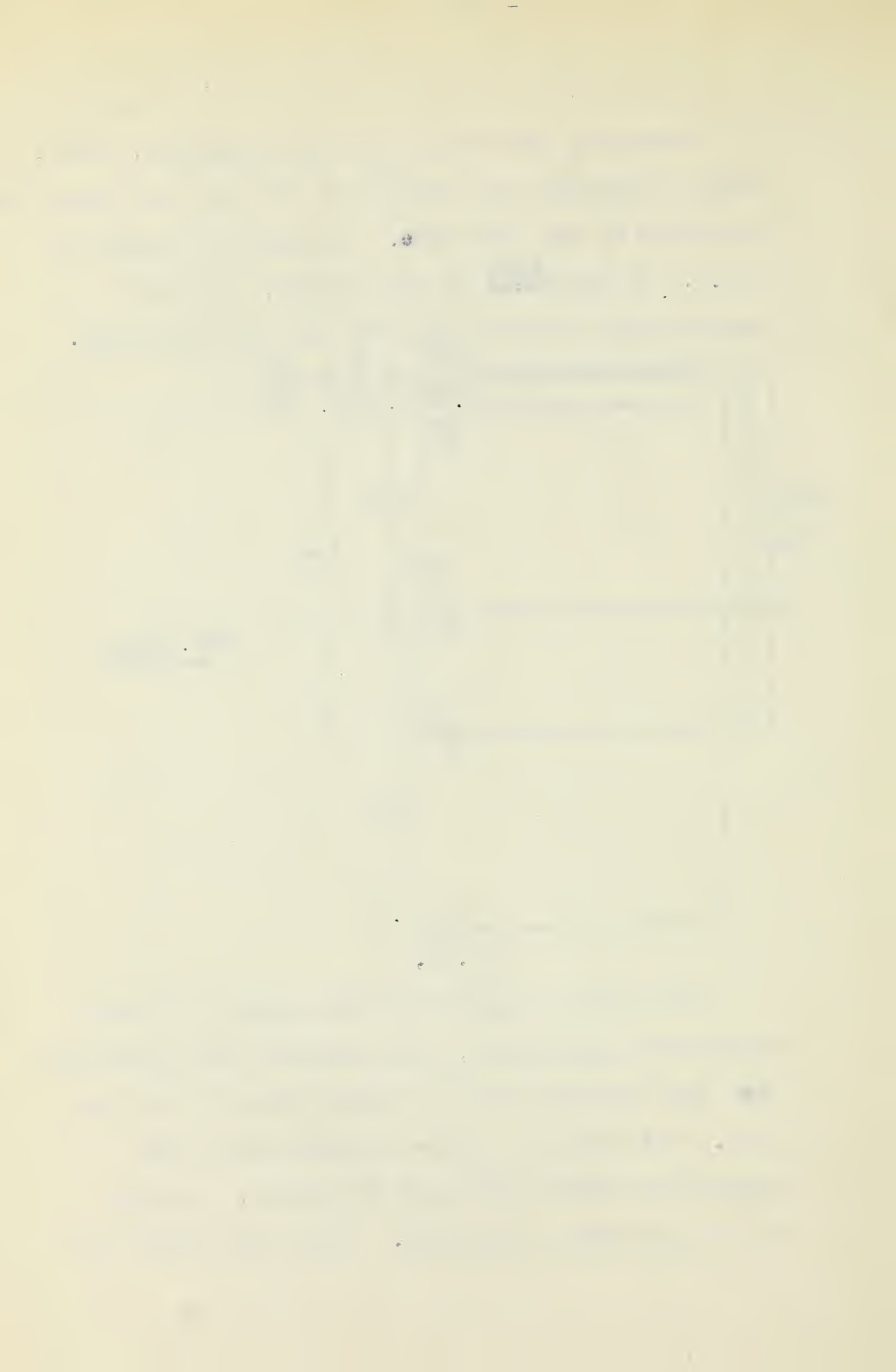


FIG. 8.

This rather complicated arrangement of levels may not be unambiguous, since each of the separations has been obtained from an examination of only one line. But there is further evidence as to the separation between $3p^2\ ^3F_2$ and 3F_3 levels, although of an approximate character. Ellis and Sawyer (g)



separated these through the lines $\lambda 4292, \lambda 4291$, giving a value of about 5 cm^{-1} . These lines are classified

as $\lambda 4292.72 \quad 6p^2 \text{ } ^3\text{P}_2 - 7^3\text{F}_2$

$\lambda 4291.72 \quad 6p^2 \text{ } ^3\text{P}_2 - 7^3\text{F}_3$

From $\lambda 2801$, the ^{hyperfine} separation of $^3\text{F}_3$ is 0.56 and from

(j), the separation of $^3\text{P}_2$ is 0.557 . Thus we should

expect the two components of $\lambda 4291.72$ to be

unresolved on the line spectrum, and we may say that

$\lambda 4291.72$ arises from the transition $6p^2 \text{ } ^3\text{P}_2 - 7^3\text{F}_3$.

Since the separation of $^3\text{F}_2$ (by $\lambda 2780$) is large, we

expect that the weaker line $\lambda 4292$ must be the

strongest component of the transition $^3\text{P}_2 - ^3\text{F}_2$, i.e.

$$6p^2 \text{ } ^3\text{P}_2 - 7^3\text{F}_2.$$

Hence, the wave number separation of $\lambda 4291, \lambda 4292$

gives us $\frac{3}{2}\text{F}_3 - \frac{3}{2}\text{F}_2 \approx 5 \text{ cm}^{-1}$.

Also, the line $\lambda 2705$ ($6^1\text{D}_2 - 7^3\text{F}_{2,3}$) was found on

the line spectrum, and consisted of two components

with a separation of about 4.7 cm^{-1} . The components

to be expected for this line in order of decreasing intensity are

$$6^1\text{D}_2 - 7^3\text{F}_3$$

$$6^1\text{D}_2 - 7^3\text{F}_2$$

and

$$6^1\text{D}_2 - 7^3\text{F}_1$$

Now $\Delta(6^1\text{D}_2) = 0.834$ by (i)

$$\Delta(7^3\text{F}_{2,3}) = 0.56 \text{ by } \lambda 2801$$

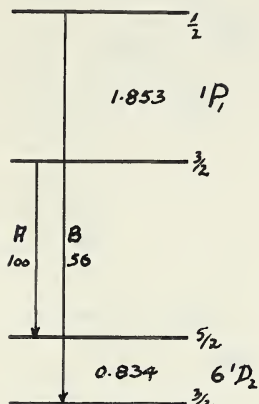
Hence these two components would not be resolved and we have the value 4.7 for the separation $7\frac{3}{2}F_3 - 7\frac{3}{2}F_2$.

Although these checks are only approximate, they do indicate the correct order of magnitude, a necessary check when working with Lummer plates.

These levels form a good example of what is to be expected when the nuclear spin interaction energy is of the same order as the spin-orbit interaction. Needless to say, it is useless to attempt to reconcile the observed separations with any formulae under THEORY, since we there assumed that the nuclear interaction was small as compared to the spin-orbit interaction. There is one interesting feature about the diagram of 3F levels (fig.8). According to the perturbation theory, two neighboring levels with the same f value should exert a repulsive effect upon one another. This effect is quite evident in the case of the two levels with $f=\frac{5}{2}$ and the two with $f=\frac{7}{2}$.

$\lambda 2948$ $6'D_2 - 9'P_1$

$$\Delta(6'D_2) = 0.834 \text{ (i)}$$



<u>Plate</u>	<u>B - A</u>
Q6	2.691
Q4	2.684
<u>Q6</u>	<u>2.685</u>
Av.	2.687 \pm .003

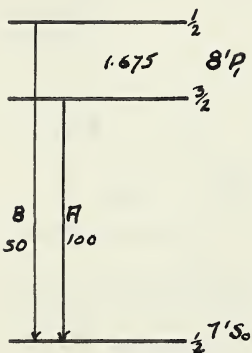
$$\Delta(9'P_1) = -1.853$$

The line $\lambda 2948$ was resolved on the line spectrum and the observed separation agrees approximately with the above.

.....

$\lambda 3029$ $7'S_2 - 8'P_1$

$$\Delta(7'S_2) = 0$$



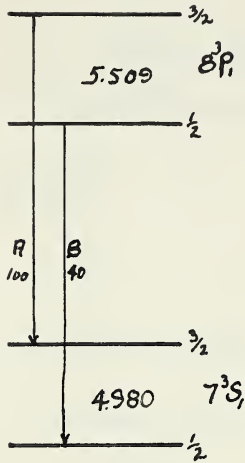
<u>Plate</u>	<u>B - A</u>
Q6	1.675
Q4(blend)	1.658
<u>Q6</u>	<u>1.675</u>
Av.	1.675

$$\Delta(8'P_1) = -1.675$$

This was also measured on the line spectrum in agreement with the above result.

$\lambda 2928 \quad 7^3S_1 - 8^3P_1$

$\Delta(7^3S_1) = 4.980 \text{ (i)}$



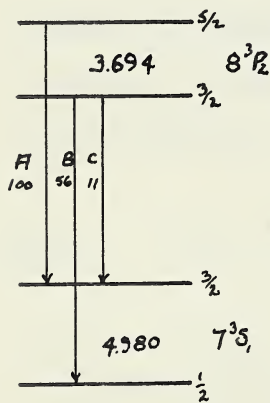
<u>Plate</u>	<u>A - B</u>
Q4	0.521
Q6	0.535
<u>Q4</u>	<u>0.532</u>
Av.	0.529 \pm .005

$\therefore \Delta(8^3P_1) = 5.509$

.....

$\lambda 2849 \quad 7^3S_1 - 8^3P_2$

$\Delta(7^3S_1) = 4.980 \text{ (i)}$

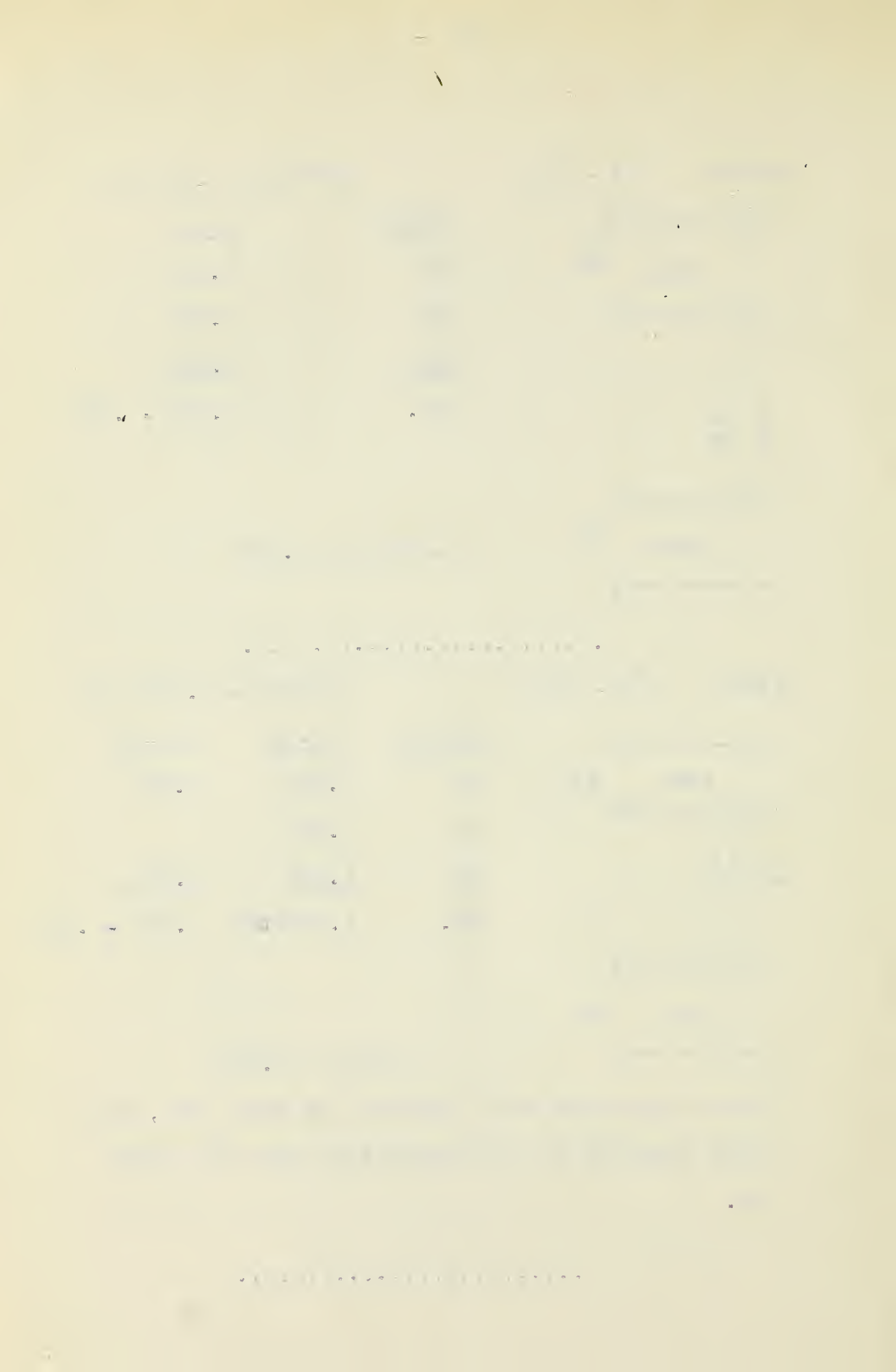


<u>Plate</u>	<u>B - A</u>	<u>A - C</u>
Q4	1.284	3.683
Q4	1.286	
<u>Q6</u>	<u>1.292</u>	<u>3.711</u>
Av.	1.287 \pm .005	3.697 \pm .014

$\Delta(8^3P_2) = 3.694$

Three components were observed for this line, the third checking the interpretation from the other two.

.....



$\lambda 2806$ $7'S_0 - 11_1$

$$\Delta(7'S_0) = 0$$

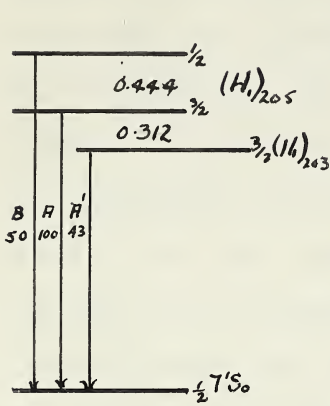


Plate	<u>B - A</u>	<u>A - A'</u>
Q6	0.439	0.309
Q4	0.449	0.315
Q4	<u>0.444</u>	<u>0.312</u>
Av.	0.444 \pm .003	0.312 \pm .002

$$\Delta(11_1) = -0.444$$

Isotope shift of (11_1) -0.312

It was impossible to ascertain a difference in the intensities of the components B and A. This makes the above interpretation ambiguous. However, judging by isotope shifts observed previously (i) (j), for terms of this configuration, the direction of shift should be negative.

.....

$\lambda 3243$ $7'P_1 - 9'D_2$

$$\Delta(7'P_1) = -1.277 (j)$$

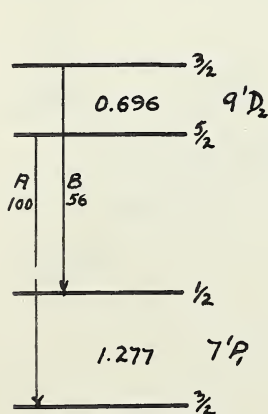


Plate	<u>A - B</u>
Q4	0.587
Q4	0.570
Q6 (blend)	<u>0.6</u>
Av.	0.581 (The first measurement is doubly weighted.)

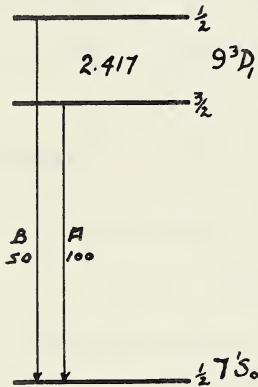
$$\Delta(9'D_2) = -0.696$$

The component A was very broad on both Q4 and Q6

plates, and unresolved from B on the Q6 plate. This made the determination of the separation A - B difficult, for it was impossible to tell whether or not there was overlapping of the fringes. An examination of the line $\lambda 2973$ ($^3P_1 - 9^1D_2$) was made on the line spectrum. It was too faint to measure on the strongest interferometer plates. Two components were observed leading to a value of -0.74 for the separation of 9^1D_2 . This lead to the more accurate value -0.696 above.

.....

$\lambda 2987$ $7^3P_0 - 9^3D_1$ $\Delta(7^3P_0) = 0$



<u>Plate</u>	<u>B - A</u>
Q6	2.419
Q6	2.416
<u>Q4(blend)</u>	<u>2.404</u>
Ave.	$2.417 \pm .002$

$$\Delta(9^3D_1) = - 2.417$$

The line $\lambda 2987$ was resolved and the separation B - A measured on the line spectrum to check the above value.

.....

Λ3004 $7^3P_1 - 9^3D_2$

$$\Delta(7^3P_1) = 4.015 \text{ (j)}$$

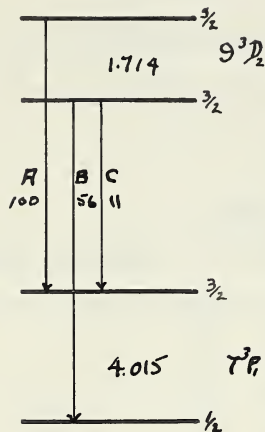


Plate	B - A	A - C
Q6	2.301	1.731
Q4	2.294	
Q6	2.292	
Q4	2.308	
Av.	2.301 ± .005	1.731

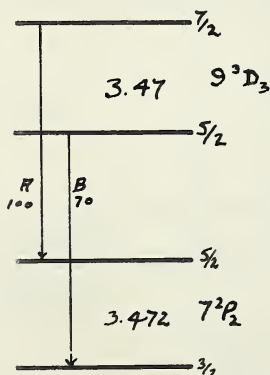
$$\Delta(9^3D_2) = 1.714$$

The component C was very faint and measureable only one plate. The difference A-C gives $\Delta(9^3P_2)$ directly but because of the intensity of C, measurement of the separation A-C is not very reliable.

.....

Λ3238 $7^2P_2 - 9^3D_3$

$$\Delta(7^2P_2) = 3.472 \text{ (i)}$$



$$\Delta(9^3D_3) = 3.47$$

The line consisted of a single broad component. Hence the separation of 9^3D_3 must be approximately the same as (7^2P_1) .

.....

$$\lambda 2941 \quad 7^3P_1 - 10^3D_3 \quad \Delta(7^3P_2) = 3.472 \text{ (i)}$$

This line consisted of a single component on all plates examined. Hence the separation of the level 10^3D_3 is 3.47 .

.....

Table of Level Separations

Configuration	Levels	H.F.S. Separations in cm^{-1}	Interaction Constant $A \text{ cm}^{-1}$
6s7f	1F_3	1.773	The fine and hyperfine structure of these levels is presented to best advantage in fig.8.
	3F_2		
	3F_3		
	3F_4		
6s8p	1P_1	-1.675	
	3P_0	0	
	3P_1	5.509	
	3P_2	3.694	
6s9p	1P_1	-1.853	
6s9d	1D_2	-0.696	-0.279
	3D_1	-2.417	-1.607
	3D_2	1.714	0.686
	3D_3	3.47	0.992
6s10d	3D_3	3.47	
$5d^2 6s^2 6p$	11,	-0.444	
	Isotope Shift $(\frac{3}{2}11) - (\frac{3}{2}11)_{2.03}$	-0.312	

Calculations of Nuclear g-Factor.

Of those investigated, the only configuration for which the terms and levels are known to be in the right order is the 6s9d. Although the known levels of 6s8p are too, the 3P_0 level has not been located, and the 1P_1 level is badly perturbed by the level 8^0_1 (see Ellis and Sawyer (g)). Hence we shall calculate g values from the data of the 6s9d configuration only, not taking into consideration perturbation effects.

Using the 1D_2 level as a reference, the energy difference in cm^{-1} between the levels of the 6s9d configuration are obtained from (g) and given below.

$$\begin{aligned} W(^1D_2) &= 0 \\ W(^3D_3) &= -294 \\ W(^3D_2) &= -353 \\ W(^3D_1) &= -381 \end{aligned} \quad \dots\dots\dots (35)$$

Hence, by equations (30) and (31) we obtain

$$\begin{aligned} \mathcal{L} &= 34.8 \\ G_0 &= 164.4 \end{aligned} \quad \dots\dots\dots (36)$$

We note that $\frac{1}{2}\mathcal{L}$ should be equal to the Landé interval factor for the 3D term, if the coupling were strictly (LS). The values of $\frac{1}{2}\mathcal{L}$ derived directly from (35) are 19.7 and 14 with an average 16.9. This forms a rough check on the calculations.

With the above value for \mathcal{J}_d , we can evaluate $(\overline{I_3})$ in the approximation of equation (9). We have $(\overline{I_3}) = \frac{hc \times 34.8}{2 \times 81 \mu_0^2} \cdot (\frac{6}{5})$ where the factor $\frac{6}{5}$ is the relativity correction H.

If we compare the magnitudes of $a(j)$ and $a(s)$, using the expressions on p.20; the above value for $(\overline{I_3})$ and Racah's (s) value of 2340 for $8\pi \frac{\mu_0^2}{hc} \psi^2(\theta) F$, we see that

$$a(2+\frac{1}{2}):a(s) \sim 1:50,000$$

$$a(2-\frac{1}{2}):a(s) \sim 1:50,000$$

Thus it is clear that the d electron contributes little to the splitting of the 3D levels, and for calculations of g to three figures, may be left out of consideration.

For the 9^3D_3 level, we apply the formula (32) with neglect of the d electron and get

$$g(I) = \frac{3 \times [A(^3D_3)] \times 1838}{2340} = 2.34$$

$$\text{where } \frac{8\pi}{5} \frac{\mu_0^2}{hc} \psi^2(\theta) F = 2340.$$

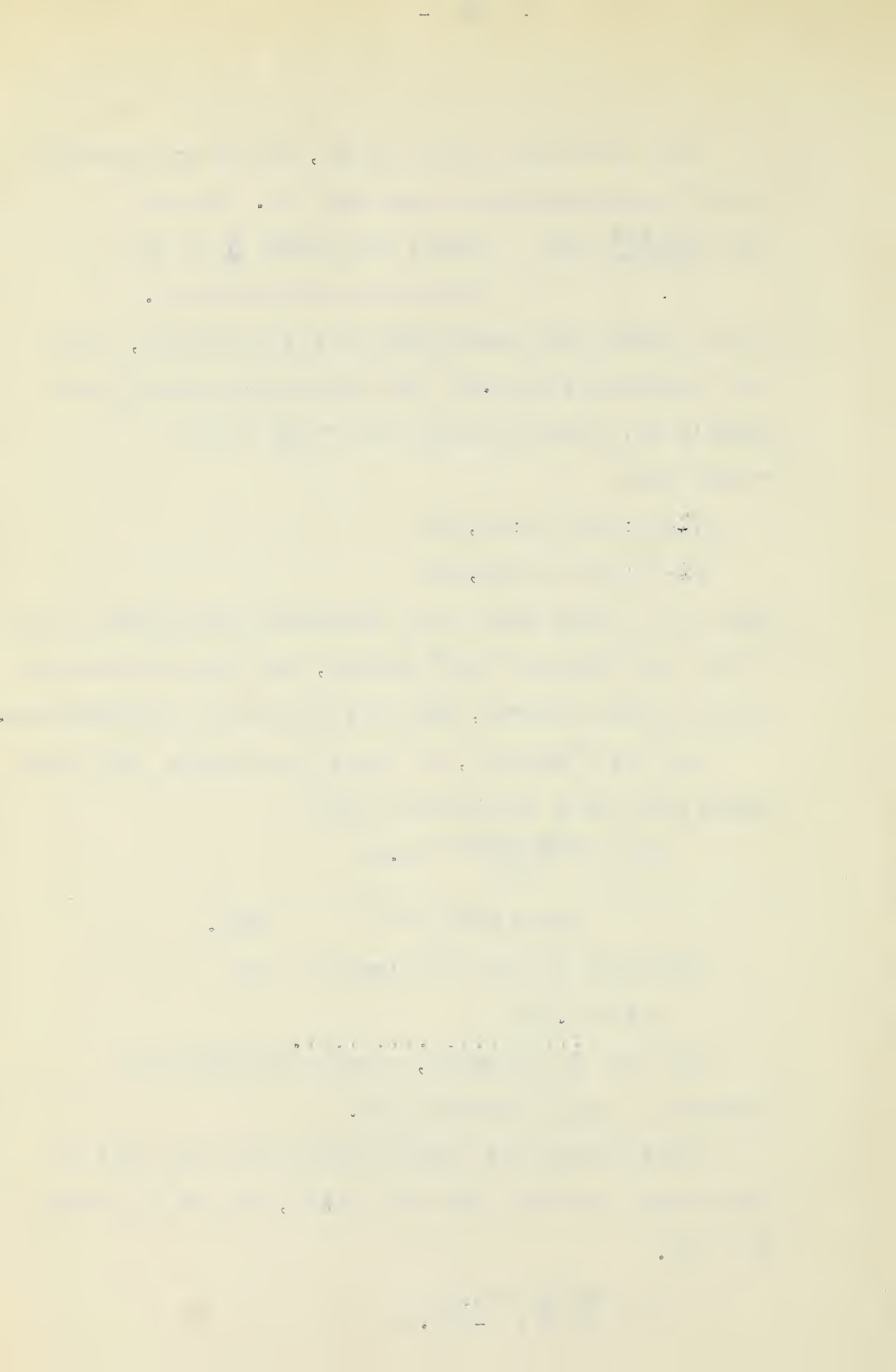
Similarly for the 9^3D_1 level we get

$$g(I) = 2.53$$

For the $^1D_2, ^3D_1$ levels, we must evaluate the constants c, c_2 of formula (34).

Substituting the results (36) into that part of the secular equation (28) for $J=2$, we get two roots of ϵ viz.

$$\begin{aligned} \epsilon &= W(^1D'_2) = 5.2 \\ &= W(^3D'_1) = -351.3 \end{aligned}$$



Then by (31') and the first root of ϵ i.e. 5.2, we have

$$\frac{K_1}{K_2} = 8.19$$

Normalizing the K's we get

$$\begin{array}{ll} K_1 = 0.1213 & K_1^2 = 0.0147 \\ K_2 = 0.9926 & K_2^2 = 0.9853 \end{array}$$

Then by (26) we get the c's

$$\begin{array}{lll} \text{i.e.} & c_1 = 0.534 & c_1^2 = 0.285 \\ & c_2 = 0.845 & c_2^2 = 0.714 \end{array}$$

Substituting these into (34), and using Racah's value for $\frac{8\pi}{3} \mu_0^2 \psi^2 \phi F$ we get

$$g(I) = 2.06 \text{ for the } ({}^3D_2) \text{ level.}$$

$$g(I) = 2.30 \text{ for the } ({}^1D_2) \text{ level.}$$

Altogether then, we have from the 6s9d configuration the values

<u>Level</u>	<u>$g(I)$</u>
1D_2	2.30
3D_3	2.34
3D_2	2.06
<u>3D_1</u>	<u>2.53</u>
Av.	2.31

Comparing these values with those of Table VI of Smith and Convey (j), we see that the values of $g(I)$ derived from the n^3D_1 and n^3D_3 levels increase with n .

Since for all of these levels, the contribution of the d electron is small compared to s electron, it appears that the calculated values of $a(s)/g(I)$ are in error. A correct determination ought to take into consideration the screening effect of the d electron.

It is rather difficult to account for the low value of $g(I)$ obtained from the 3D_2 level, for it is not near to any term likely to perturb it. On the other hand, the value of $g(I)$ derived from the 1D_2 level is in good agreement with the values of Smith and Convey (j), even though the 1D_2 level is distinctly perturbed by the $6p^2\ ^1D_2$ level (see Ellis and Sawyer(g)). Of course, the hyperfine splitting of this level is small, and hence it should not greatly affect the splitting of the $9d\ ^1D_2$ level.

ACKNOWLEDGMENTS

I am happy to have this opportunity to express my appreciation of the guidance, assistance and kindly interest extended by Prof. Stanley Smith during the prosecution of this research. I am also indebted to the other members of the Physics Department and to Dr. Boomer of the Chemistry Department for suggestions and advice.

May I also extend my thanks to Mr. Gleave and to Mr. MacFarlane for making up and repairing apparatus as it was required. The liquid air used in the experimental work was always promptly supplied by Dr. Boomer and Mr. Thomson of the Chemistry Department.

I am very grateful to the University for the award of a University of Alberta Research Scholarship. Without this financial assistance it would have been impossible to devote my full time to the problem at hand.



